STRATAL ARCHITECTURE AND SEDIMENTOLOGY OF A PORTION OF THE UPPER CAMBRIAN HICKORY SANDSTONE, CENTRAL TEXAS, U.S.A.

A Thesis

by

ISAAC ANTONIO PEREZ TERAN

Submitted to the Office of Graduate Studies of
Texas A&M University
in partial fulfillment of the requirements for the degree of

MASTER OF SCIENCE

August 2007

Major Subject: Geology

STRATAL ARCHITECTURE AND SEDIMENTOLOGY OF A PORTION OF THE UPPER CAMBRIAN HICKORY SANDSTONE, CENTRAL TEXAS, U.S.A.

A Thesis

by

ISAAC ANTONIO PEREZ TERAN

Submitted to the Office of Graduate Studies of
Texas A&M University
in partial fulfillment of the requirements for the degree of

MASTER OF SCIENCE

Approved by:

Co-Chairs of Committee,	Brian Willis
	Arnold Bouma
Committee Member,	Walter Ayers
Head of Department,	John Spang

August 2007

Major Subject: Geology

ABSTRACT

Stratal Architecture and Sedimentology of a Portion of the Upper Cambrian Hickory Sandstone, Central Texas, U.S.A. (August 2007)

Isaac Antonio Perez Teran, B.S., Universidad de los Andes

Co-Chairs of Advisory Committee: Dr. Brian Willis
Dr. Arnold Bouma

Fluvial and coastal depositional environments may have been quite different before the development of land plants in the late Silurian. Rapid drainage of terrestrial surfaces, flashy rivers with poorly stabilized banks, coarse sediment loads supplied to coasts from landscapes dominated by physical weathering, and the prevalence of epicontinental seas are expected to have altered depositional patterns and associated preserved Facies. Quarries in the Upper Cambrian Hickory Sandstone located in central Texas provide an exceptional opportunity to examine the sedimentology of deposits of this age in order to interpret sedimentary environments. During quarrying, vertical walls, one half-kilometer long and several tens of meters high, are blasted back a few tens of meters at a time and then the rubble excavated, exposing successive outcrops in walls that are perpendicular to the regional paleocurrent direction. The deposits are characterized by sheet-like bedsets dominated by unidirectional cross-stratified sandstones interpreted to have formed in coastal areas fed by bedload dominated rivers. Thinner heterolithic and clay beds locally separating cross-stratified bedsets are commonly bioturbated by marine organisms. Presence of tidal features, such as abundant mud drapes, concave-upward cross-stratification and sparse herringbone cross-stratification, also suggests marine influence during deposition. Detailed mapping of stratal geometry and Facies across these exposures shows a complex internal architecture that can be interpreted in terms of growth and superposition of bars within shallow fluvial channels and adjacent shallow marine areas along the coast. Detailed 3D reconstruction of bars and channels reveals a range of processes including growth, coalescence, and erosion of bars during channel migration, switching and filling of channel segments, and mouth bar growth as channelised flows decelerated seaward. Sedimentary Facies, stratal geometry and ichnofossils suggest that these deposits were formed in a braid-delta system fed by low-sinuosity bedload-dominated rivers. Basinal processes were controlled by the shallow epicontinental sea, dissipating wave action and strengthening tidal currents.

ACKNOWLEDGMENTS

I like to thank many people that have made the culmination of this thesis possible. First of all, I thank my committee chair, Dr. Brian J. Willis. He has been a constant support and has gone above and beyond the call of duty on many occasions. I really appreciate his patience, encouragement, efforts and his invaluable input to this project. In addition, I want to thank my committee members, Dr. Arnold Bouma, and Dr. Walter Ayers for their help and for being here today. I also would like to acknowledge the former co-chair of my project, Dr. Brann Johnson, who couldn’t be part of my committee due to retirement but who played a crucial role in the development of this project. Thank you Brann for all the time you spent taking pictures and helping surveying the quarry walls, and most importantly, thank you for your constant advice not only as a professor but also as a personal friend.

Special thanks to my office mates Rafael Almeida and Fernando Rodriguez. Rafael has been like a brother to me during my time at Texas A&M, and together with Fernando made the office time a really pleasant and enjoyable experience. Sergio, Pablo, Ezequiel, Pablo Cervantes, Martin and others have always been a great support. Thanks guys!

Thanks to all my family, especially my parents, brother and sister, for their constant moral and financial support.

Last, but not least, I would like to thank my girlfriend Kell for her love, patience and support during this time. I feel lucky to be with such a wonderful person.

TABLE OF CONTENTS

Page

Page

LIST OF FIGURES

FIGURE Page

INTRODUCTION

Early Paleozoic terrestrial and shallow marine depositional environments may have been significantly different than those that characterize times after the widespread development of land plants. Drainage from barren landscapes would have been flashier and watersheds more rapidly denuded. High rates of surface erosion clog rivers with bedload sediment resulting in dominantly braided river channel patterns. Braid plains of channels with high width to depth ratios, unstable banks, and rapid channel switching form broad sand sheets rather than narrower channel belts encased in overbank muds (Cotter 1978; Macnaughton et al. 1997). Without plants, aeolian processes can more efficiently winnow sediment, moving silt- and clay-sized sediments offshore leaving clean aeolian-reworked sands in terrestrial areas. Rapid shifting of river courses also influences deposition along shorelines, resulting in a dominance of braid-delta morphologies. Early Paleozoic shelves probably had broad, gentle, seaward slopes in general due to the prevalence of epicontinental seas, in contrast with the narrower, steeper, shelves that dominate modern continental margins (Eriksson et al. 1998).

Interpreting depositional environments from Precambrian and early Paleozoic deposits has proven to be problematic because most deposits of this age are reported to be comprised of sheet-like beds of sandstone that are difficult to divide into distinct fluvial and marine systems tracts. Key diagnostic criteria like paleosols in terrestrial deposits and rich patterns of bioturbation in marine strata did not form. There is also a lack of well exposed deposits of this age that have not been deformed. Those deposits that are well preserved generally reflect deposition within craton interiors where

---

This thesis follows the style of the Journal of Sedimentary Research.

transitions between terrestrial, shoreline and shelf environments occur gradually across the margins of low-gradient epicontinental seas. There is a need for more examples of these age deposits; particularly examples that are sufficiently exposed to allow details of the bedding architecture and Facies to be examined and interpreted in terms of depositional processes within different depositional settings.

The Hickory Sandstone Member of the Riley Formation is a well known Cambrian sandstone in central Texas (Cornish 1975; Kim 1995; Krause, 1996; Wilson 2001). The lower part of this sandstone is a transgressive succession that passes upward from a fluvial incised disconformity surface into sandstone-dominated deposits that have been interpreted to be fluvial, becoming interbedded marine sandstones and mudstones. Thus, this sandstone should record transitions from fluvial, shoreline, to open marine depositional Facies, and potentially contain a record of cyclic shoreline regressions and transgressions. Although the Hickory Sandstone is remarkably undeformed and unaltered by diagenesis, it is regionally poorly exposed and crops out only in small natural outcrops and isolated road cuts. This study examines quarry exposures of the lower to middle Hickory Sandstone near Brady, Texas. The highwall in this quarry, over a half-kilometer long and 20 meters high, allows details of Facies distribution and stratal architecture within this portion of the Hickory Sandstone to be documented for the first time. The highwall was excavated back in lateral steps of a few tens of meters during this study, and bedding diagrams constructed from successive parallel quarry walls provide a unique record of Facies variations in three dimensions. These retreating quarry

These retreating quarry walls provide an exceptional opportunity for the analysis of early Paleozoic sedimentary processes and environments.

EARLY PALEOZOIC DEPOSITIONAL ENVIRONMENTS

Recognition and interpretation of early Paleozoic depositional environments has proved difficult due to differences in the nature of sedimentary processes prior to the advent of land plants and differences in the early ocean-atmosphere chemistry, the biosphere, and in the style of plate tectonics (Eriksson et al. 1998).

During the late Cambrian North America occupied an equatorial position, and therefore probably had a tropical, wet climate (Fig. 1). Atmospheric CO_2 concentrations were considerably higher during the early Paleozoic than today, producing an enhanced greenhouse effect (Berner 1993). This CO_2-rich atmosphere may have increased chemical weathering rates (Eriksson et al. 1998). The lack of both vegetation cover and humic soils also promoted physical weathering, erosion and transport of sediments from source areas (Hiscott et al. 1984). High rates of weathering would have rapidly denuded uplands and increased rates of sediment supply to basins.

Aeolian processes are effective erosional agents without the binding, sheltering, and moisture retaining functions of vegetation. Long distance aeolian transport of fine sediments may have been particularly enhanced before land plants developed. Dalrymple et al. (1985) analyzed the geographic distribution of Cambrian-Ordovician shales in North America and postulated that most of the silt and clay blown from Cambrian and Early Ordovician land areas was carried westward by a prevailing easterly trade winds across the equatorial region of North America. On the basis of this idea they suggested that the present-day northeasterly section of the North America craton was a zone of net removal of fines, and southern and western sections were areas of net accumulation.

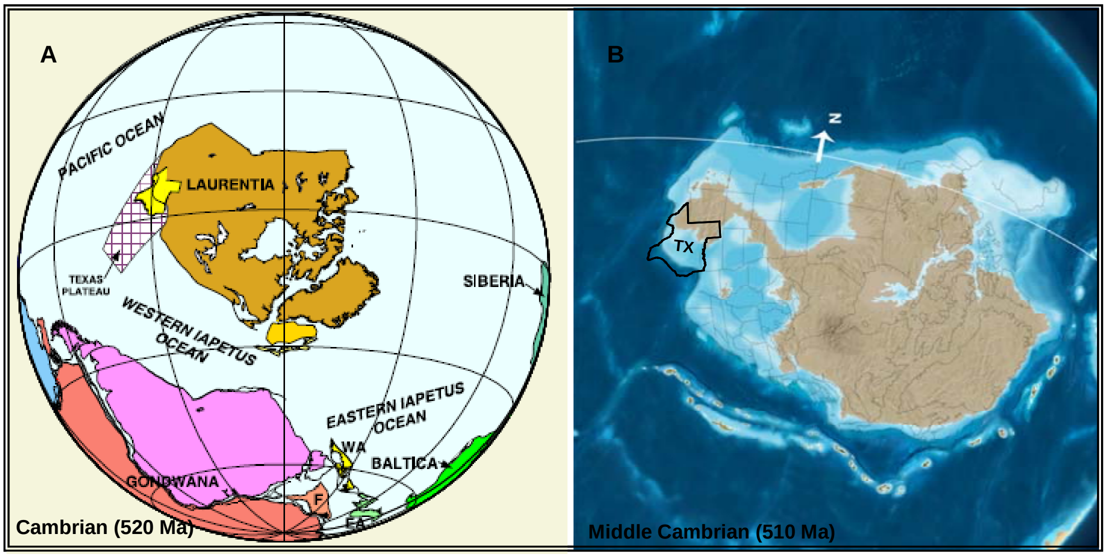

Fig. 1. A) Paleogeographic reconstruction of the middle Cambrian (520 million years).The Texas Platform was located near the equator. (Modified from Dalziel and Gahagan 2006, PLATES project web page, The University of Texas at Austin). B) Possible distribution of the epicontinental sea around the Laurentia continent (modified from Dr. Ron Blakey web page, Northern Arizona University).

Eriksson et al. (1995) suggested that aeolian deflation of drainage basins may not have been as pronounced as implied by Dalrymple et al. (1985), on the basis of thick mudrock accumulations they interpreted to be directly offshore of braid-delta and peritidal sheet sandstone accumulations.

Fluvial depositional processes are significantly influenced by land plants. The lack of vegetation would result in high river discharge variability, high rates of discharge decline following major floods, and high sediment yield resulting in bed-load dominated streams (Sonderholm and Tirsgaard 1998). Rapid fluctuations in discharge may be one reason why evidence for more stable meandering stream deposits is rare. A lack of fine material left following aeolian reworking would have favored bedload-dominated rivers. Plant growth can strongly influence channel bank strength because of pervasive root reinforcement and because a layer of exposed roots can provide a protective bank covering (Smith 1976). Vegetation also could indirectly enhance bank resistance by inducing deposition of fine-grained sediments in vegetated areas (Knighton 1984) and could anchor or cover the sediment on floodplains, inhibiting channel reoccupation (Schumm 1985). The lack of land plants in pre-Silurian times would have led to decreased channel bank stability, yielding braidplains of rapidly switching channels with high width/depth ratios, and high sand to mud ratios (Cotter 1978). Modern shallow, wide, braidplain channel deposits in arid areas comprise broad sheet-like sand bodies.

Epeiric seas were probably common during the Proterozoic (Eriksson et al. 2002) and the early Paleozoic (Fig. 1). The break up of Rodinia would have been associated with abundant plate spreading centers, rapid production of new warm oceanic crust and generally high sea levels. Epicontinental seaways inundated large portions of cratonic terranes and appear to have been characterized by shelf-like environments that extended far from shelf margin breaks. Such broad shallow seas may have amplified asymmetrical tidal currents and dampened open ocean wind-formed waves. Estimation of bathymetry in ancient epeiric seas is difficult. Although widespread Phanerozoic carbonate deposits suggest areas with depths less than 30 meters, phosphate nodules in black shales in other areas suggest the possibility of depths greater than 100 meters (Eriksson et al. 1998). A lack of modern examples makes interpretation of epicontinental sea deposits problematic (Irwin 1965; Brenner 1980; Bouma et al. 1982, Eriksson 2002).

Late Precambrian and early Paleozoic shoreface deposits are reported to have typical tide- and wave-generated sedimentary structures like hummocky-swaley cross-stratified, parallel laminated, and trough and planar cross-bedded sandstones. Several authors have inferred tens to hundreds of meters thick successions composed uniformly of 10-30 cm thick planar and trough cross-beds to be shoreface deposits (Eriksson et al. 1998). The great thickness of these deposits relative to modern shoreline examples were interpreted to reflect more uniform or permanent ocean circulation patterns combined with a delicate balance between subsidence and sediment influx (Soegaard and Eriksson 1989). Descriptions of barrier islands with associated washover fans and lagoons in pre-Silurian deposits are rare. The lack of examples of these types of deposits may be related to significant erosion during transgression of broad shallow shelves, rapid channel switching of coastal rivers in the absence of land plants, or the lack of muds to define distinct lagoonal Facies (Macnaughton et al. 1997).

Tide-dominated coastal environments may have been favored relative to modern times given the board extent of shallow epicontinental seas (Tape et al. 2003). Tirsgaard (1993) suggested that Precambrian tidal channel deposits differ from their modern counterparts in that they had very low mudstone content (even within environments today characterized by heterolithic deposits) and relatively abundant high energy deposits. Thus characteristic upward-fining successions may not have been widely developed. He suggested that like fluvial channel deposits of this age, tidal deposits are dominantly sand sheets formed during rapid lateral migration of intertidal channels. Tidal flat deposits may not have been muddy.

Although tide-influenced deposits during pre-vegetation times should have diagnostic features of tidal action (e.g., numerous reactivation surfaces and discontinuous mud drapes within cross sets, herringbone cross-stratification, presence of ebb and flood caps, and undulatory lower set boundaries associated with successive bundles of foresets), tides may have been more rotary within broad submerged cratonic areas, generating more unidirectional currents at any one location. This contrasts with modern analogs, where in most locations tidal wave rotation onto cratons is blocked by land areas, and thus becomes more rectilinear toward coasts as tides flood and drain the land with each passing tidal wave. The lack of local tidal current reversals and potentially less mud traveling with sand in tide-influenced areas may make differentiation between sandy tidal channel and ephemeral fluvial deposits difficult. Low subsidence rates within shallow cratonic seas may also lead to low preservation rates, further hindering this distinction (Soderholm and Tirsgaard 1998). Lack of obvious tidal indicators in early Paleozoic successions led some investigators to conclude that epicontinental seas were too shallow to transmit significant tidal energy from the open ocean to flooded continental interiors (Irwin 1965), or that tidal currents were not strong enough to transport sand near coasts (Keulegan and Krumbein 1949). Tape et al. (2003), however, documented tidal bundling in a lower Paleozoic sheet sandstone in the cratonic interior of North America, showing that tides were significant along some inboard areas of Cambrian coastlines. An alternative is that some areas of shallow epicontinental seas may have had the correct dimensions to generate tidal resonance, significantly increasing tidal range and strengthening tidal currents along some areas of the shoreline and not others.

Delta deposits have been identified in late Proterozoic and early Paleozoic clastic successions based on Facies associations and vertical lithological profiles similar to modern examples. These similarities suggest deltaic sequences were controlled broadly by the same deposition processes associated with decelerating currents offshore (Eriksson et al. 1998). The absence of vegetation may have favored braided distributary networks and the rapid switching of mouth bars. Rapidly shifting river mouths would lead to braid-deltas created by sandy braided streams debouching into a shallow sea (McCormick and Grotzinger 1993), rather than birds-foot delta morphology with thick capping interdistributary bay successions (MacNaughton et al. 1997). In low gradient epeiric seas, thin, relatively-sandy, mouth-bar successions may be broadly sheet-like. High sediment supply and efficient alluvial sediment transport before vegetation also may have promoted thick deltaic deposits (Eriksson et al. 1998).

HICKORY SANDSTONE

The Hickory Sandstone, Late Middle to Late Cambrian in age, comprises fluvial, shoreline, and marine strata deposited during the transgression of shallow seas on the Texas platform. This area was a passive continental margin during Cambrian time located at the western edge of the proto-North America (Laurentia) craton next to the Iapetus Ocean (Fig. 1). The Hickory Sandstone was deposited into the landward end of a shallow epicratonic embayment (Krause 1996). Paleogeographic reconstructions show that during the Middle Cambrian, Laurentia was near the equator (Fig. 1). The presence of paleosols on Precambrian surfaces beneath the Hickory Sandstone suggests deposition in an area with a tropical, wet climate (Brann Johnson, Personal Communication 2007).

The Hickory Sandstone is the basal member of the Riley Formation. It is overlain successively by the Cap Mountain Limestone and Lion Mountain Sandstone Members of the Riley Formation (Cloud et al. 1945) (Fig. 2). The Riley Formation unconformably overlies a topographically complex unconformity created by differential erosion of northwest to southeast trending, tightly-folded, Precambrian gneiss and schist, and granitic intrusions (Fig. 3; Stenzel 1935). Hickory Sandstone onlaps this unconformity surface and thus varies in thickness across central Texas from absent where there are paleotopographic highs to approximately 168 meter thick in the deepest paleotopographic lows (Barnes and Bell 1977). Cross-bed paleocurrent directions within the Hickory Sandstone record the influence of this erosional paleotopography, demonstrating a clear northwest to southeast control on early Riley Formation sediment transport (Wilson 1962; Cornish 1975; Krause 1996). The regional paleogeographic and

Era	System	Group	Formation	Member or unit
Paleozoic	Ordovician	Ellenberger Group	Honeycut Formation	Undivided
			Gorman Formation	Undivided
			Tanyard Formation	Staendebach Member
				Threadgill Member
	Medium to upper Cambrian	Moore Hollow Group	Wilberns Formation	San Saba Member
				Point Peak Member
				Morgan Creek Limestone Member
				Weldge Sandstone Member
			Riley Formation	Lion Mountain Sandstone Member
				Cap Mountain Limestone Member
				Hickory Sandstone Member
Precambrian	Valley Spring Gneiss/Packsaddle Schist/Town Mountain Granite			

Subunits
Upper Hickory
Medium Hickory
Lower Hickory

Fig. 2. Stratigraphic column of central Texas, USA. (modified from Krause 1996).

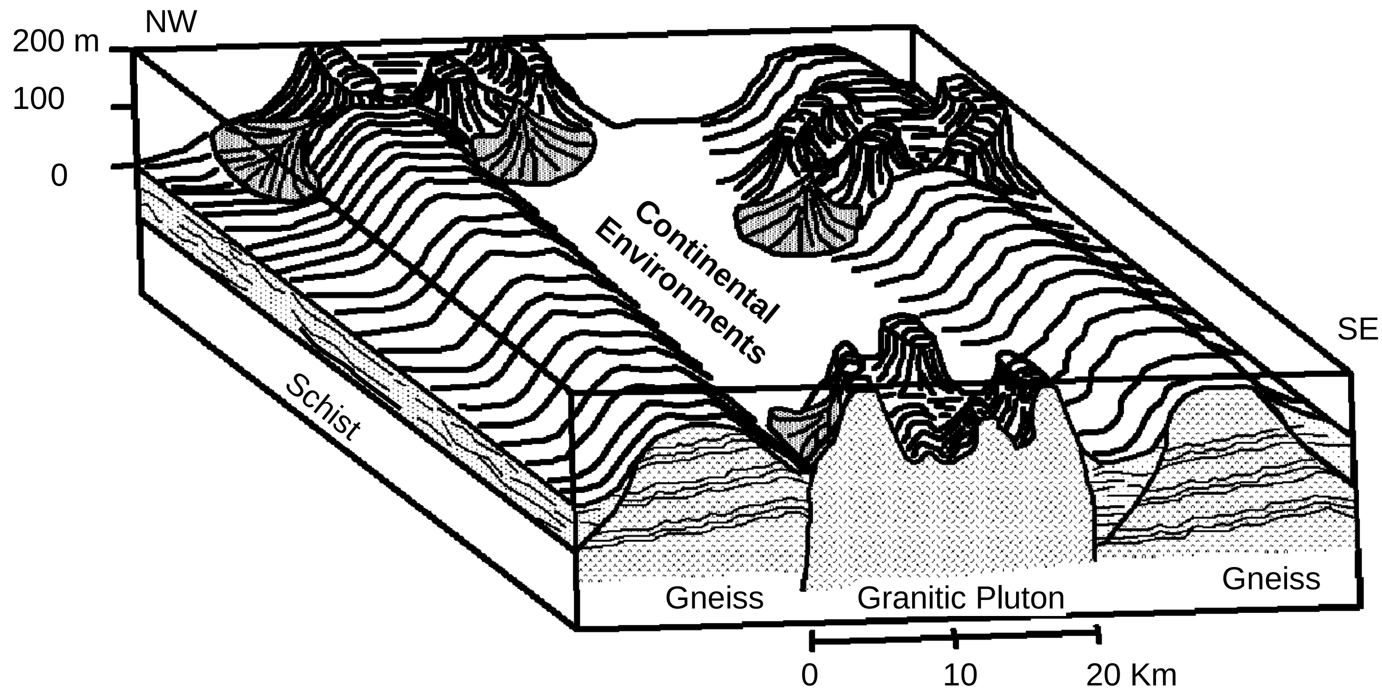

Fig. 3. Diagramatic representation of Precambrian erosional surface prior to the Hickory Sandstone deposition in the Texas cratonic embayment. Ridge-and-swale topography resulted from the diferential erosion of the folded, less resistant Packsaddle schists and more resistant Valley Spring Gneisses. Younger granitic intrusives have more resistant marginal zones (modified from Krause 1996).

stratigraphic setting and framework-grain composition of the Hickory indicate that detritus came from the Central Texas Craton and areas to the northwest (Barnes et al. 1959; Wilson 1962). McBridge et al. (2002) suggest that Hickory detritus was derived primarily from granitic rocks and associated pegmatites and secondarily from gneisses, schist, and silicified volcanic rocks.

The Hickory Sandstone is subdivided into the upper, middle and lower subunits (Fig. 2). It is a broadly transgressive succession that grades upward from fluvial to shallow marine deposits. The basal sandstones of the lower Hickory have been interpreted to be braided stream deposits, which grade upward into tidal flat and intertidal estuarine deposits (Goolsby 1957; Cornish 1975; Krause 1996). The overlying middle Hickory consists of fluvial-influenced, shallow subtidal estuarine and shoreface deposits (Krause 1996). The upper Hickory is interpreted to be estuarine channel-shoal deposits to shallow, high energy, open marine deposits (Cornish 1975, Krause 1996).

The 45 to 70 meter thick lower Hickory Sandstone is composed primarily of cross-bedded, coarse to medium-grained, angular to subangular, poorly sorted quartzose sandstones with occasional finer grained sandstones and mudstone intervals (Bridge et al. 1947; Barnes and Bell 1977). The appearance of continuous, moderately to extensively bioturbated, mudstone beds mark the transitional contact between the lower and the middle Hickory Sandstone. The 55 to 70 meter thick middle Hickory is better sorted than the lower Hickory and contains less large-scale cross-bedding. It consists of fine- to medium-grained sandstones and bioturbated mudstones (Barnes and Bell 1977; Randolph 1991, Wilson 2001). It has been informally divided into more mud-rich lower middle Hickory and a somewhat sandier upper Middle Hickory (Johnson 1997). The contact between the middle Hickory and upper Hickory is marked by an increase in hematite cement and appearance of hematite ooids (Barnes and Schofield 1964; Barnes and Bell 1977). The Upper Hickory is typically 15 to 30 meters thick (Barnes and Bell 1977) and is characterized by coarse grained, moderately well sorted, well rounded quartz sandstone with iron-oxide ooids and cement interbedded with occasional orangish-white, fine grained sandstones and dark maroon mudstones (Barnes and Schofield 1964; Randolph 1991; Wilson 2001).

Different subunits and Facies have been defined by previous studies of the Hickory Sandstone and interpreted in terms of sedimentary environments (summarized in Table 1). Differences in interpretation may in part reflect the widely distributed nature of outcrops and cores used in different studies. Regional studies were generally based on composite sections from several localities and limited small outcrops, which hindered paleo-environmental reconstructions (Wilson 2001). Wilson (2001) also suggested that the variety of interpretations of the lower Hickory is due to the paleotopography of the Precambrian basement, which had local effects on depositional environments and was onlapped by deposits of different age. Based on Facies variations described in previous studies, and cores that penetrate the Precambian basement a few miles from the study area, the deposits discussed in this project are located in the upper part of the lower Hickory Sandstone.

Table 1. Summary of previous studies of the Hickory Sandstone compiling different interpretations of Stratigraphy and depositional environments (Modified from Wilson, 2001)

Study	Data	Stratigraphic Subdivisions			Depositional environments
Bride et al. 1947	Outcrop	Two mappable units based on aqueous or aeolian deposition			Aqueous with possible aeolian deposits in basal portion of Hickory.
Goolsby 1957	Outcrop	Three mappable units:	Upper Hickory	B	Offshore shallow marine
				A	Nearshore shallow marine
			Middle Hickory		Shallow marine, possibly tidal in part
			Lower Hickory		Braided stream to deltaic
Cornish 1975	Outcrop and Core	Six Distinct facies:	Laminated Calcite sandstone		Storm dominated shelf transitioning into carbonate shelf
			Even bedded sandstone		Storm dominated shelf near influence of tidal shoals
			Hematitic sandstone		Estuarine channel-shoal complex
			Siltstone facies		Inner estuarine point bar and muddy intertidal flats
			Burrowed sandstones		Tidal flat and intertidal bars
			Basal cross-bedded sandstone		Outer estuarine
Kim 1995	Core and Thin section	Three distinct facies:	Facies 3		Transgressive sheet sand
			Facies 2		Delta-Front
			Facies 1b		Braided stream/distributary channel
			Facies 1a		Braided stream
Krause 1996	Outcrop and Core	Six distinct facies:	Mudstone (HM)		Isolated lagoons or sheltered embayments
			Hematitic (HH)		Very shallow and high energy, normal marine
			Siltstone (HS)		Transition on very shallow subtidal inner platform between the open embayment and sand flats of the coast and basinwards oolitic shoals
			Burrowed (HB)		Shallow subtidal estuarine embayment and shoreface marginal to fluvial fed sand sheet
			Cross bedded	(HXc)	Intertidal and flats marginal to shallow estuarine embayment
				(HXb)	Channel fill and channel margin sheet flood deposits
				(HXa)	Bed-load fluvial systems
			Alluvial	(HAb)	Aggradational fan-plain to braid-plain braided stream channels
				(HAa)	Alluvial fan deposits
Wilson 2001	Outcrop, Core and Well logs	Four distinct facies:	Hematite facies (H)		Open marine environment with a strong tidal influence
			Interbedded sandstone facies (SS)		Estuarine mouth to transitional open marine
			Mudstone-rich facies	(MS2)	Middle estuarine environment
				(MS1)	Subtidal, upper middle estuarine deposits
			Cross bedded	(XB2)	Braided stream bed-load and channel fill deposits
				(XB1)	Braid-plain braided stream channels

METHODS

The study area is part of the Oglebay Norton Industrial Sands' Brady quarry operation located near Voca, Texas in southern McCullock County, Texas (about 12 miles from the town of Brady, Texas; Fig. 4). Within the quarry an east-west oriented high wall is about 500 meters long and 20 meters high. The strike of this quarry wall is highly oblique to the regional southeast paleocurrent directions reported for the Hickory Sandstone (Wilson 1962; Cornish 1975; Krause 1996). The strata exposed in this quarry dip a few degrees to the north and are deformed only by sparse faults with offsets generally less than a few meters. The east-west quarry high wall is excavated northward in stepped segments, blasting the east part first, then the middle, and finally the western part (Fig. 5). As a result, a succession of parallel strike-orientation outcrops, spaced about 20 meters apart, were progressively exposed and then removed. This project examines four exposed positions of the east-west quarry highwall. This retreating wall was divided into nine parts, labeled HIC01 to HIC09. HIC01 was blasted and then excavated first and HIC09 last (Fig 5). Because strata dip to the north slightly, higher stratigraphic intervals are exposed as successive walls are blasted. Photos of these walls were combined into orthorectified photomosaics to provide a template for construction of a succession of parallel bedding diagrams. Strata and Facies patterns mapped across these successive parallel bedding diagrams were correlated along dip to document the 3D geometry of sediment bodies and their internal Facies variations. Methods used for construction of orthorectified photomosaics and successive bedding diagrams are detailed below.

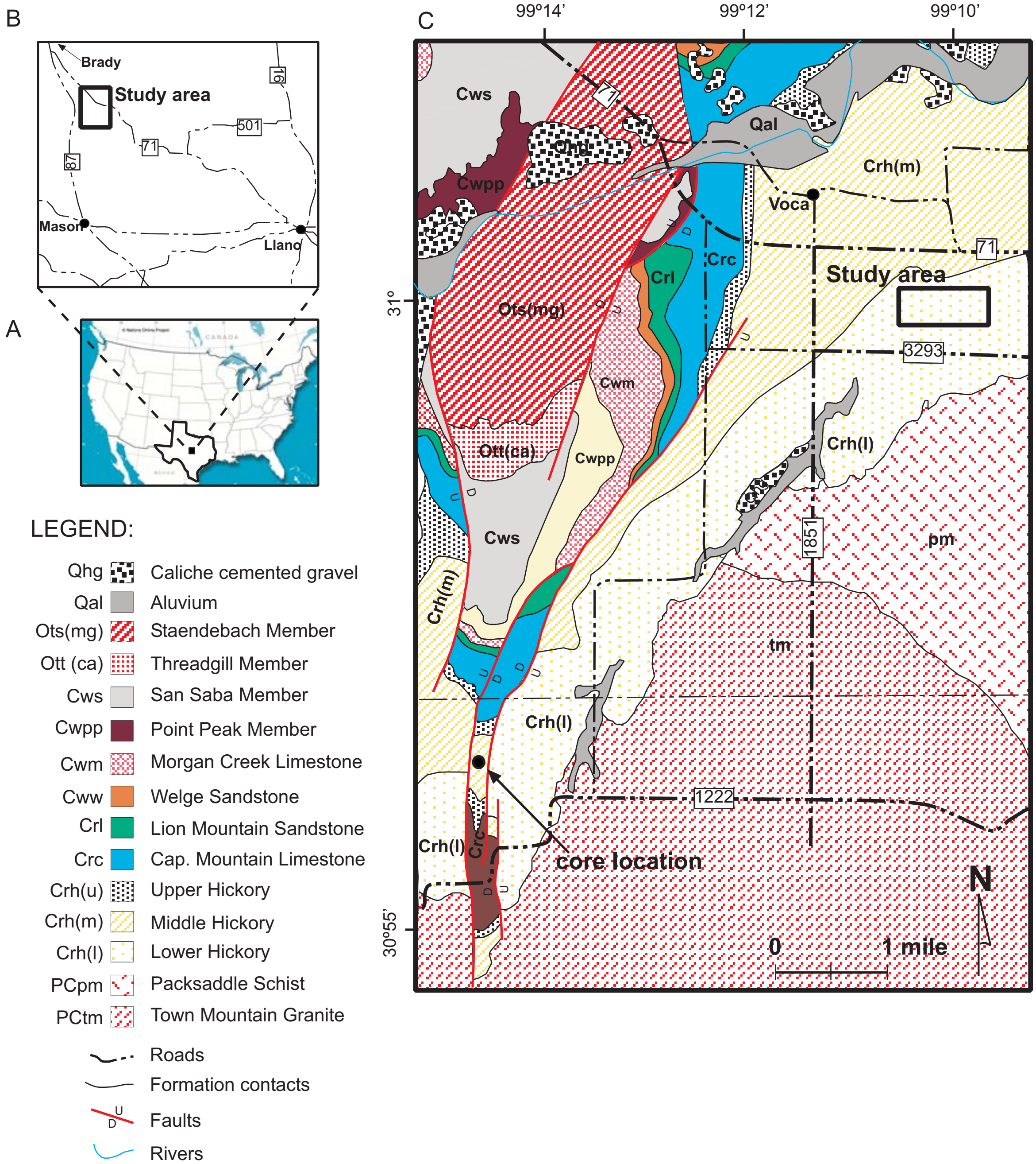

Fig. 4. Location of the study area. A) Location of Texas within North America. B) Location of the study area in central Texas. C) Geologic map of the study area (modified from Barnes and Schofield 1964). Note location of quarry (black rectangle) and the core (black dot) described in this project. Distribution of quarry walls within the quarry are shown in Figure 5. See the stratigraphic column in Figure 2 for more details of stratigraphic units.

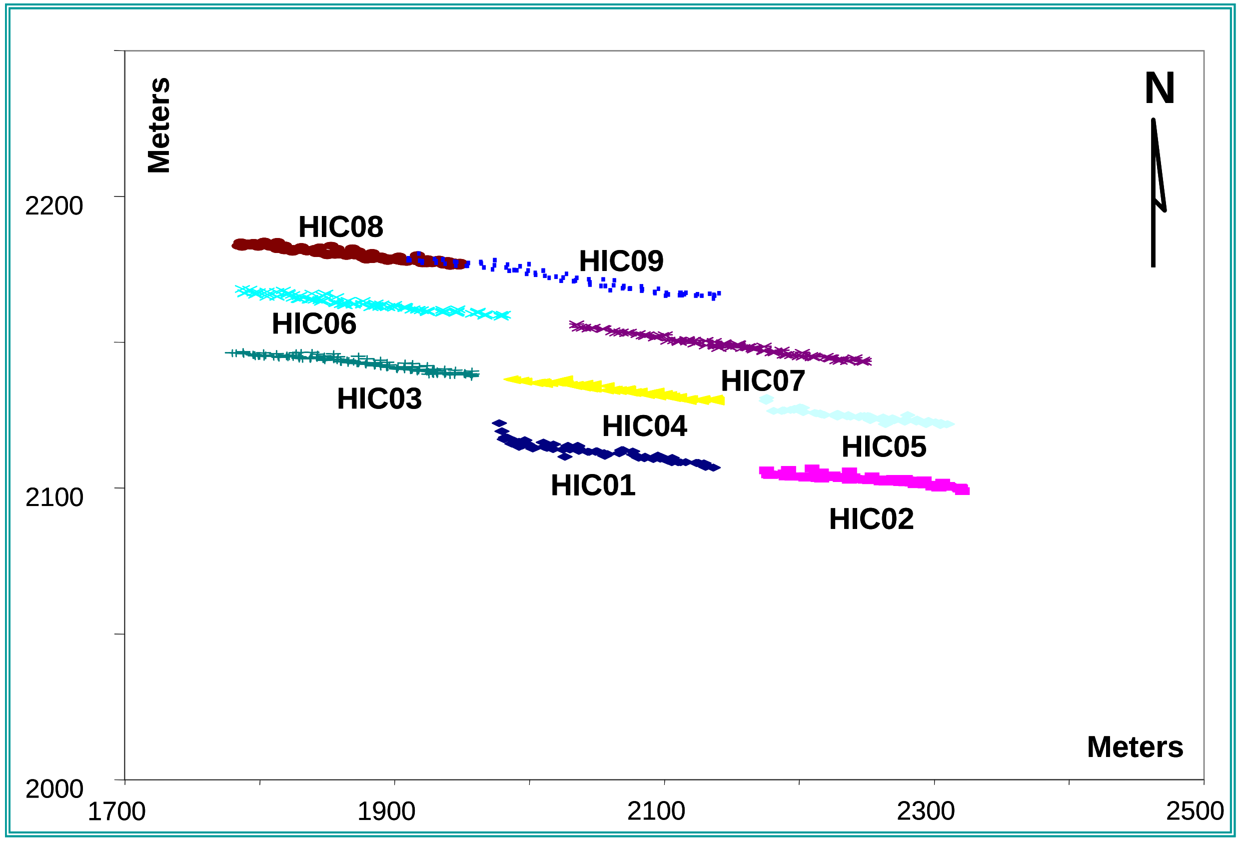

Fig. 5. Ground control points plotted in a X-Y coordinate system, showing the distribution of the different quarry walls surveyed with the total station. Note how the blasting activity was changing with time: the first two walls were blasted in three different segments (from HIC01 to HIC06), and the last two walls were blasted in two longer segments in the western side.

Construction of Orthorectified Photomosaics

Orthorectified photomosaics were constructed from high-resolution digital images to provide a base for the mapping of sedimentologic variations. Positions of points on individual photos were surveyed within a consistent 3D coordinate system using a reflectorless total station (Sokkia, series 030R). Multiple photos of each segment of quarry wall, shot from different positions, were combined with surveyed ground control points within photogrammetry software (Photomodeler) to produce orthorectified photomosaics. The photogrammetry software required photos with focal planes at a high angle (focal axis close to 90 degrees) in order to define the most accurate coordinates of unsurveyed points. It is also best to have a photograph nearly perpendicular to the outcrop face for orthoprojection. To fulfill both of these requirements, three photos of each segment of an outcrop exposure were collected. Because individual quarry walls were documented by many tens of individual photographs, photos from specific segments of the wall were modeled and orthorectified separately and then were stitched together in Photoshop for presentation. Unlike photomosaics constructed from non-orthorectified photographs, where the edges of successive photos commonly do not match up well due to differing perspective distortions, sets of photographs projected into a common plane can be aligned precisely. A two dimensional coordinate system was defined across the stitched, orthorectified photomosaics spanning each quarry wall. Because quarry walls were essentially vertical, the plane of orthorectified photomosaics and the 2D coordinate could be used together to define three-dimensional coordinates of points on the exposed quarry walls. These three-dimensional coordinates are consistent across all photomosaics of the different quarry walls documented in this study. These orthorectified photographs thus allow definition of stratal geometries in both 2D and 3D.

Defining the Hierarchy of Bedding Surfaces and Facies

Bedding diagrams were constructed by tracing bedding surfaces and polygons around distinct Facies on orthorectified photomosaics using a vector-based computer drafting program (Macromedia FreeHand 10). This mapping defined a hierarchical set of bounding surfaces, particularly discordant erosional surfaces, which show stratal geometrical arrangements and depositional patterns of sedimentary bodies. First-order surfaces bound individual trough cross-bed sets or bundles of plane-bedded laminae genetically associated with large-scale cross-strata (Fig. 6B1), and they are equivalent to the mesoscale bounding surfaces defined by Bridge (1993b). This scale was mapped only in highly detailed bedding diagrams constructed in specific areas of quarry walls but not on the larger orthorectified photomosaics where individual cross-sets were difficult to distinguish due to photographic resolution. Second-order contacts bound groups of sedimentary units of the kind delineated by first-order contacts (Fig. 6B1). These surfaces correspond the base of individual large-scale cross-strata and horizontal lamination within muddier beds. In contrast to first-order surfaces, second-order contacts were mapped on the orthorectified photomosaics as discontinuous fine-dashed lines. Third-order contacts are erosional surfaces that bound second-order scale strata sets to define individual beds (Fig. 6B1). These third-order contacts were mapped continuously to where they terminated against another surface or against the mapping border of the photomosaics. Higher-order surfaces were not recognized within this succession.

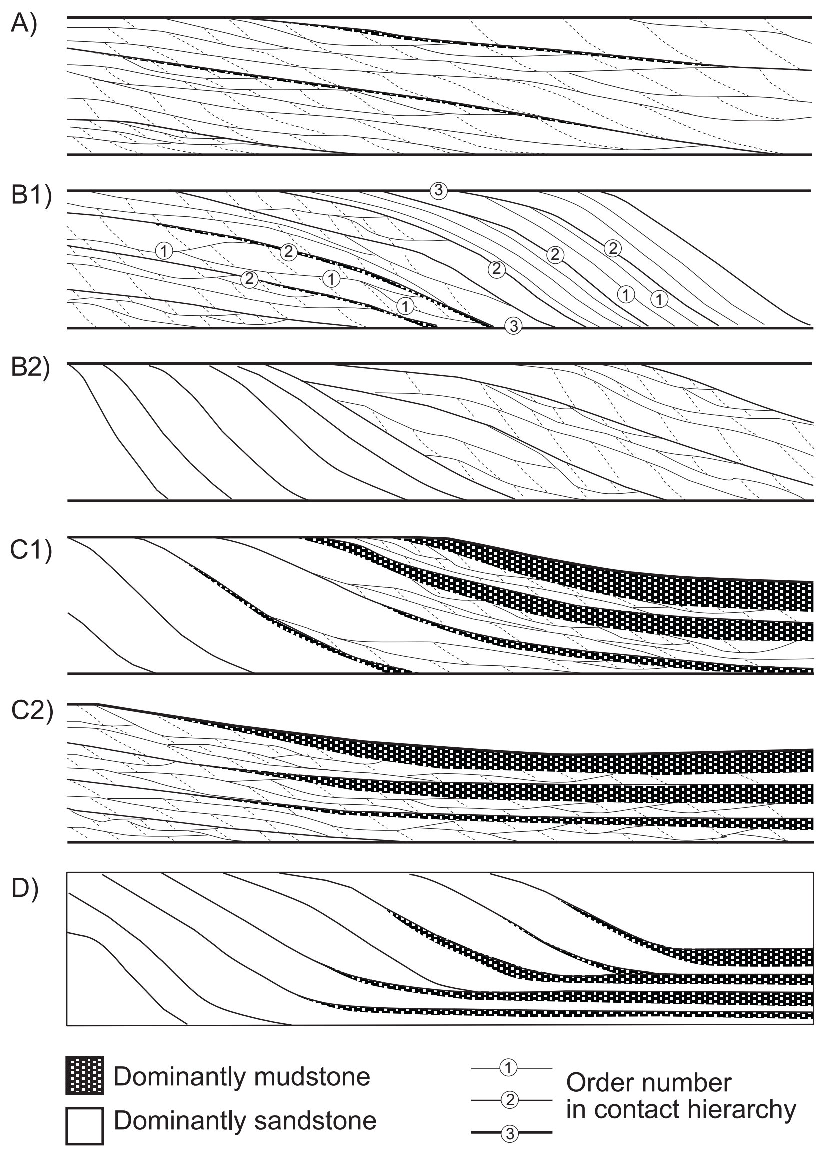

Fig. 6. Bedset diagrams showing schematic representations of bedding and Facies within each of the bedsets recognized: A) Bedset of cross-stratified cosets; B1) Bedset in which a cross-stratified coset changes laterally to a single large-scale cross-set and; B2) Bedset in which a single large-scale cross-set changes laterally into a cross-stratified coset; C1) Bedset in which sandstones of facies 2 change laterally into heterolithic deposits of facies 3; C2) Bedset in which sandstones of facies 1 grade laterally to heterolithic deposits of facies 3; D) Upward coarsening mouth bar bedset. See also different order surfaces (B1), being second and third order surfaces mapped in all bedding diagrams and first-order contacts mapped only in highly detailed localized pictures.

Facies polygons marked the location of four Facies defined principally by stratification type and grain size. Close inspection of Facies was possible only locally because direct access to the walls of this active quarry was prohibited due to safety concerns of the quarry operators. Mapped Facies were characterized by local inspection of the wall using binoculars and by identifying similar Facies within a core which is part of Wilson's (2001) data set (core labeled as NNR 4) taken a few miles from the quarry (see Fig. 4 for location and Fig. 7 for core log). Each mapped Facies is bound by a closed polygon that can cross bedding surfaces, but not other Facies polygon boundaries. Faults were also mapped to show major offsets of depositional beds. Where fault surfaces were complex they were simplified to a single line along the zone of offset. Very detailed maps of fault zone geometry within successive quarry walls were constructed for a separate study (Brann Johnson, Personal Communication 2006).

Three-Dimensional Correlations

Bedding diagrams were spatially organized within a 3D reference frame using the surveyed ground control points (Fig. 8). Bedding and Facies were defined first within quarry wall segments exposed during individual episodes of blasting and excavation to define bedding geometries, Facies assemblages, and larger scale sedimentary packages. Quarry walls along similar east-west planes were then correlated. Finally, a detailed bedding and Facies three-dimensional correlation was completed, based on three parallel wall segments along the west side of the quarry (HIC03, HIC06 and HIC08) that could be related directly to the continuous side wall of the quarry immediately adjacent to and perpendicular to these three parallel walls (Fig. 8). Continuous mud layers identified in both the three parallel walls and the side wall that could be confidently traced across these walls provided the initial framework for 3D correlation.

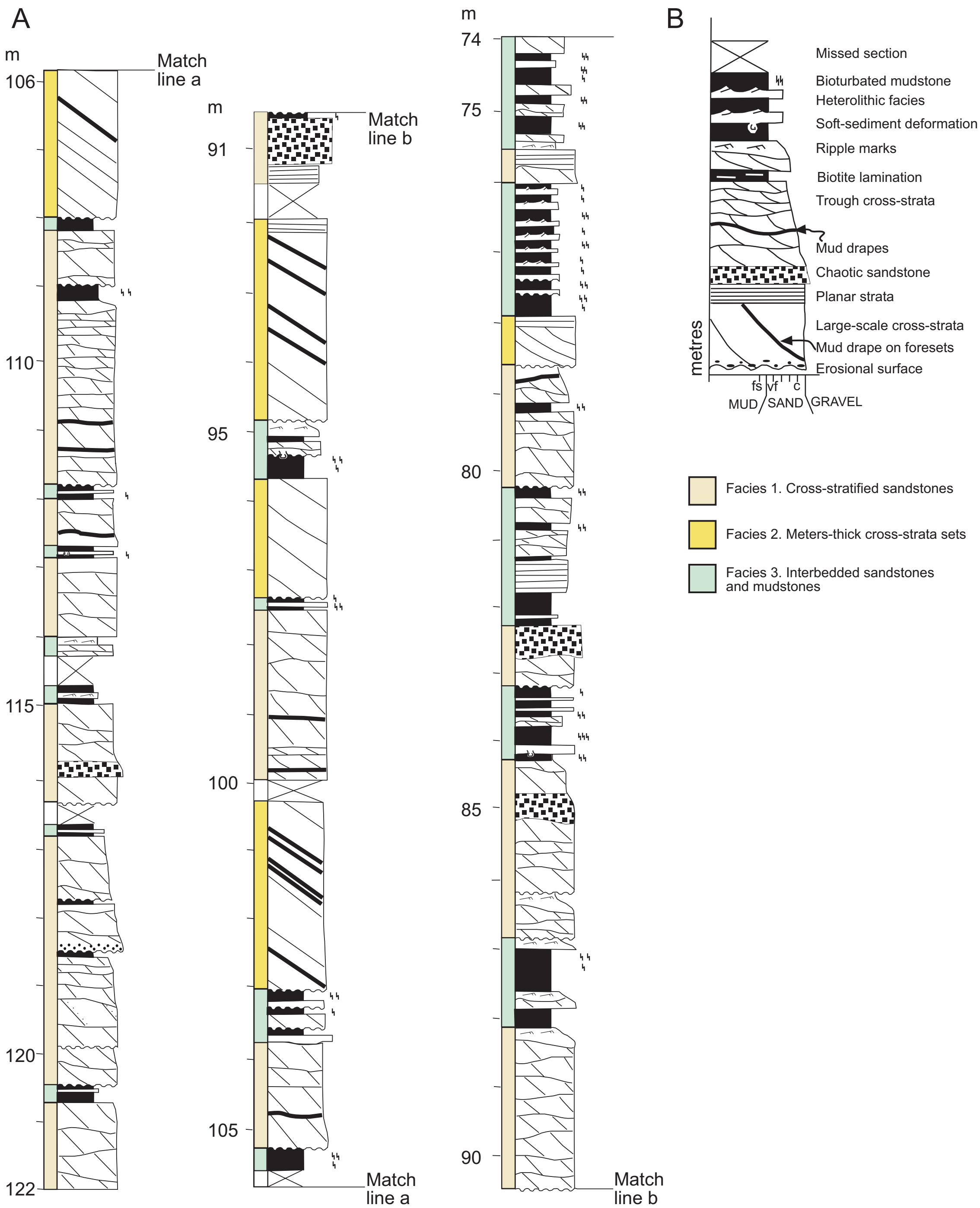

Fig. 7. Representative core that goes through the interval under study. A) Sedimentary log showing the vertical succession of facies through the lower Hickory Sandstone. Note the progressive increase in mud layers and bioturbation upward within the succession. B) Key to sedimentary logs. Location of the core can be seen in Figure 4.

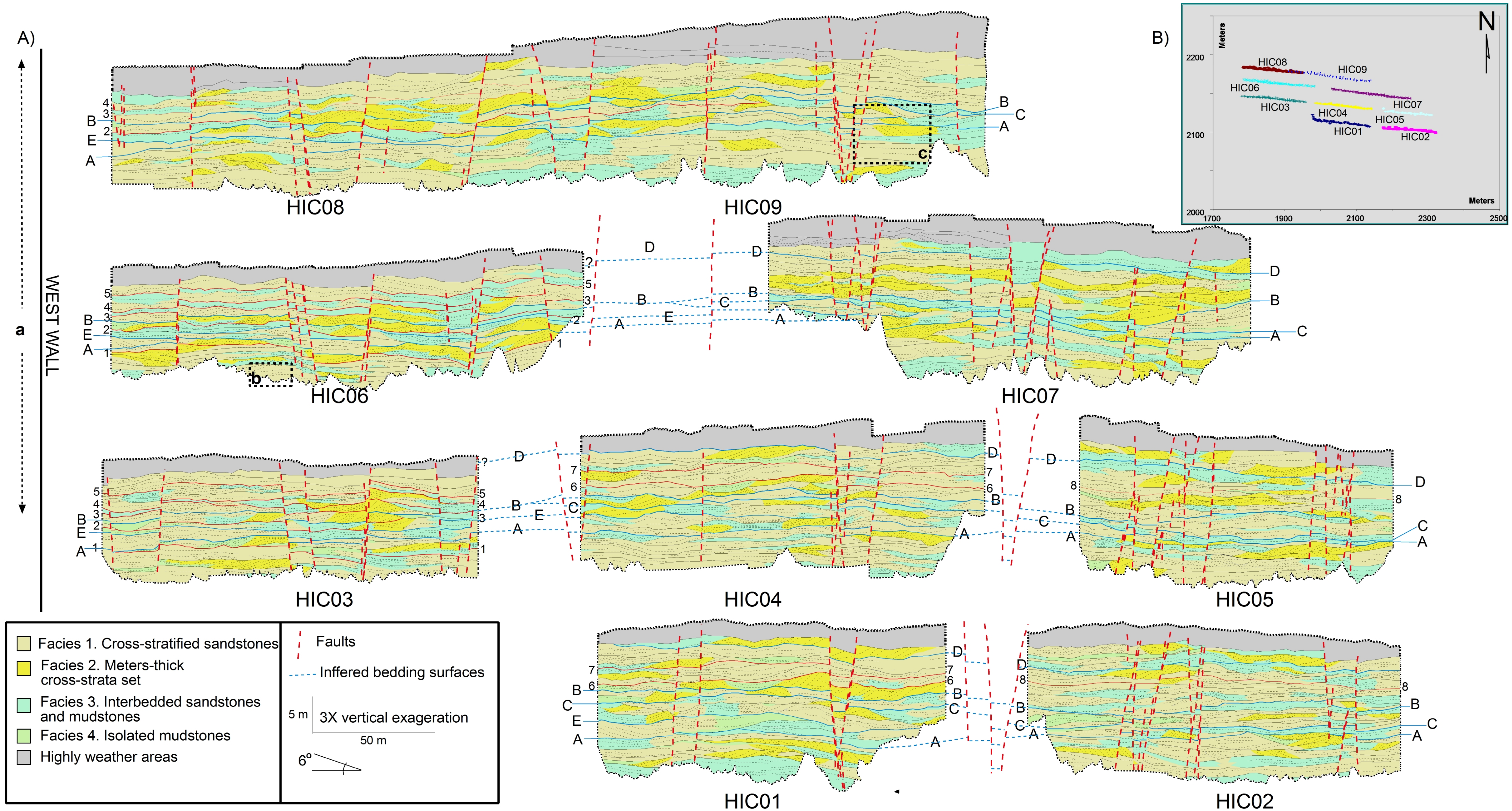

Fig. 8. A) Bedding diagrams presented within a 3D reference framework. Red lines, indicating surfaces that can be correlated among successive quarry walls are labeled with numbers. Surfaces that could be correlated between all the quarry walls are indicated by blue lines and are labeled with capital letters. Numbered capital letters represent examples of bedsets referred to in the text. Lower case letters a, b and c in dashed boxes show location of Figures 10, 11 and 12, respectively. Note that a is located at the west wall of the quarry, which is parallel to the regional paleoflow direction and perpendicular to the other quarry walls studied in this segment. B) Base map showing the map view location of the different quarry wall segments.

SEDIMENTARY FACIES

Hickory Sandstone deposits exposed in this quarry are separated into four Facies (Fig. 9). Sheet-like sandstone beds, which comprise most of the deposits, are characterized either by cross strata cosets (Facies 1) or are dominated by a single meter-thick cross set (Facies 2). Mudstone-rich deposits are classified as either Facies 3 or Facies 4. Facies description emphasizes grain size distribution and sedimentary structure variations. External geometry of the sedimentary bodies, scale, nature of the bounding surfaces and the organization and transitions between Facies within beds is addressed in a subsequent section.

Facies 1: Cross-Stratified Sandstone

Description

This Facies comprises medium- to coarse-grained sandstones, containing sets of medium- to small-scale trough cross-strata with local mudstone drapes (Fig. 9A). Cross sets are as thick as 0.5 m, but are generally 0.1-0.2 m thick. Cross-sets are lenticular in shape, characterized by an erosive concave-up lower boundary and a flat or convex-up upper boundary. Lateral extent of sets is very variable, and ranges from less than a meter to many tens of meters. Cross sets are usually more continuous in exposures oriented parallel to the paleoflow direction (Fig. 10) than in those oriented perpendicular (Fig. 11). Sets are stacked in co-sets that can be meters thick (Fig. 11C). Within the west wall, most cross strata dip toward the southeast (Fig. 10), but sets with strata dipping in the opposite direction are also observed. Detailed rose diagrams of cross strata could not be constructed due to restricted access to the quarry walls. Within most co-sets cross-strata

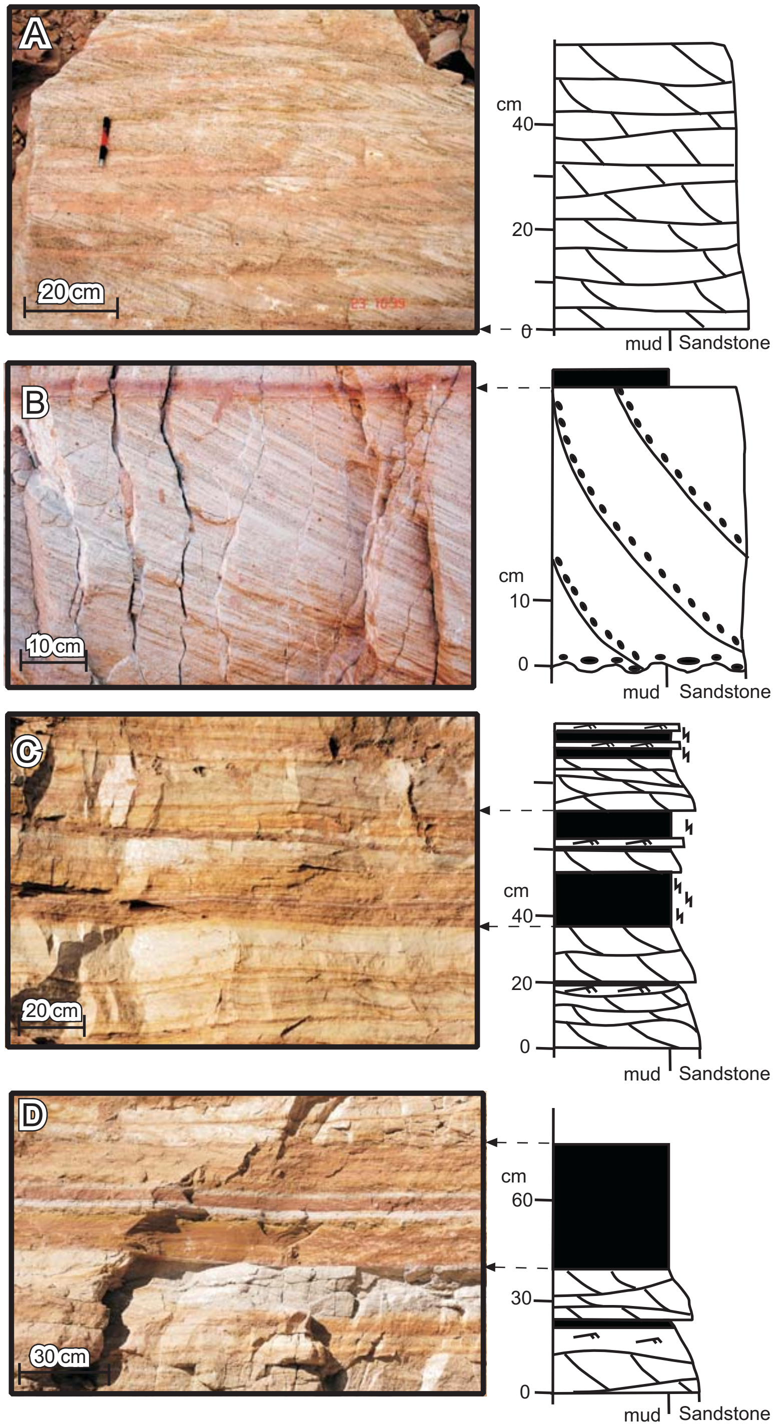

Fig. 9. Representative photographs and graphic representation of the four Facies. A) Facies 1. Cross-stratified sandstones . B) Facies 2. Meters-thick cross strata sets. C) Facies 3. Interbedded sandstones and mudstones. D) Facies 4. Isolated mudstone beds. Dashed-line arrows indicate the position of the vertical log in the picture. Key to sedimentary logs in Figure 7.

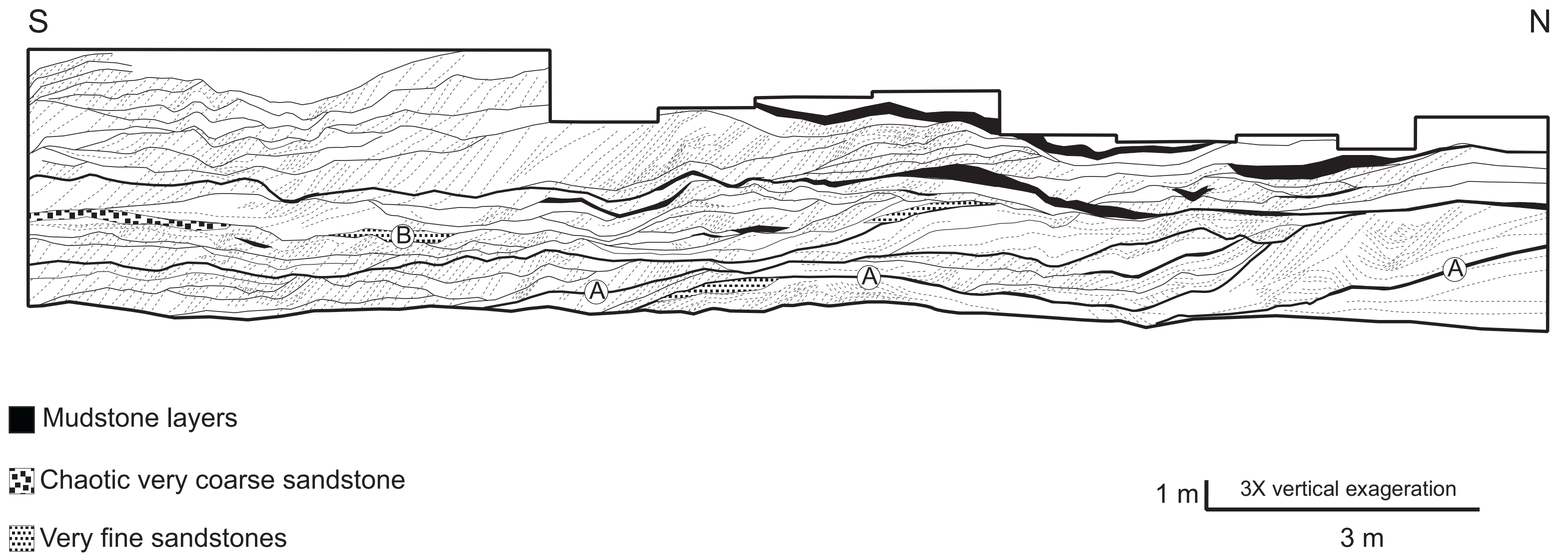

Fig. 10. Outcrop located in the west wall of the quarry, parallel to the regional paleocurrent direction (see lower case a in Figure 8 for location). This exposure records dunes migrating on top of a larger scale bedform. A) Downlapping beds progressively decrease in dip-angle defines the transition from facies 2 to facies 1 (architectural element B). B) Lateral transition from planar cross-strata to fine-grained sandstones.

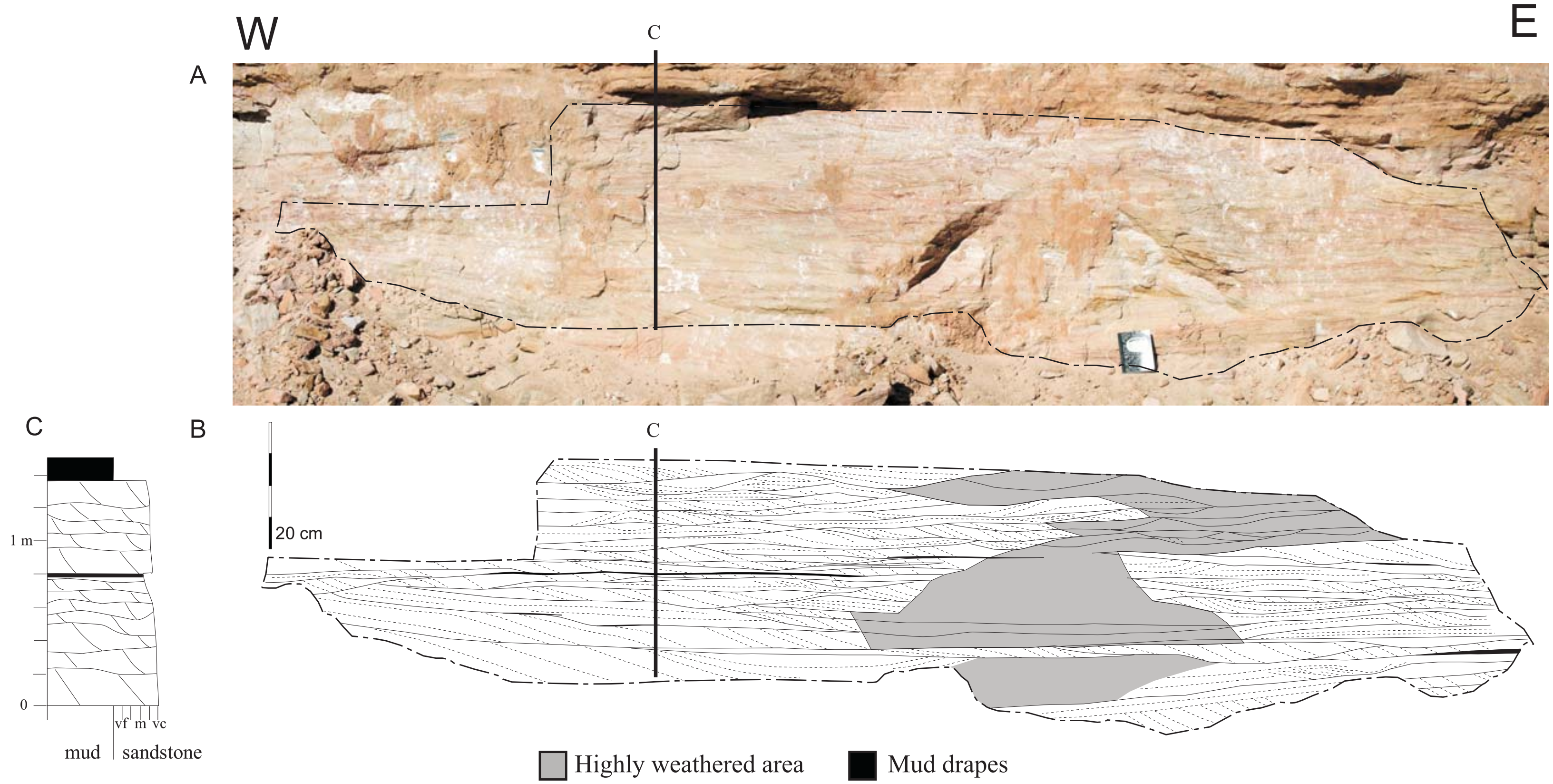

Fig. 11. A) Example of Facies 1 exposed perpendicular to the paleoflow direction. B) Bedding diagram of internal cross-stratification. C) Measured section at location C, showing a poorly defined fining-upward succession and progressive decrease in cross set thickness within bedsets. See Figure 7 for legend of the sedimentary logs and Figure 8 for location of this cross-section (lower case b).

all dip in the same direction, but a few co-sets comprise cross-strata dipping in opposite directions. Adjacent co-sets can contain cross strata with opposite dip directions.

A typical cross-stratum within a set is a few millimeters to 2 cm thick and displays normal internal vertical grain-size grading (Fig. 9A). Cross-strata are either planar, concave-upward, or rarely sigmoidal (Fig. 10). Planar cross strata are generally sandier and abut the lower set-bounding surface at a high angle. The concave-upward cross-strata, the most common shape observed, tend to be muddier, have dips less than the angle-of-repose, generally thicken upward, and have tangential contacts with the lower set-bounding surface. Mud drapes on cross strata are preserved locally, particularly in basal parts of sets. Sigmoidal cross-stratification has horizontal to low angle inclined topsets that steeppen in dip and thicken into the middle of the set. These cross strata then become thinner as they become tangential with the set's basal surface. In some cases topset strata are planar stratified or can contain smaller-scale centimeter-thick internal cross-strata sets (Fig. 12D). Occasionally toesets also contain internal smaller-scale cross-strata (Fig. 12D). Mudstone drapes are common within these cross sets.

Within a set, cross strata can be uniformly concave-upward or planar, or can change character along the set. Planar cross strata commonly passes downcurrent into concave-upward cross strata. This lateral transition is commonly associated with progressive decrease in cross strata dip angle and decrease of grain size. In other locations planar or concave-upward cross-strata passes into lower-angle sigmoidal cross-strata. When this is the case, the topset parts of the sigmoidal cross-stratification pass up-current into horizontal strata that overlay the concave-up or sigmoidal strata erosively (Fig. 12D).

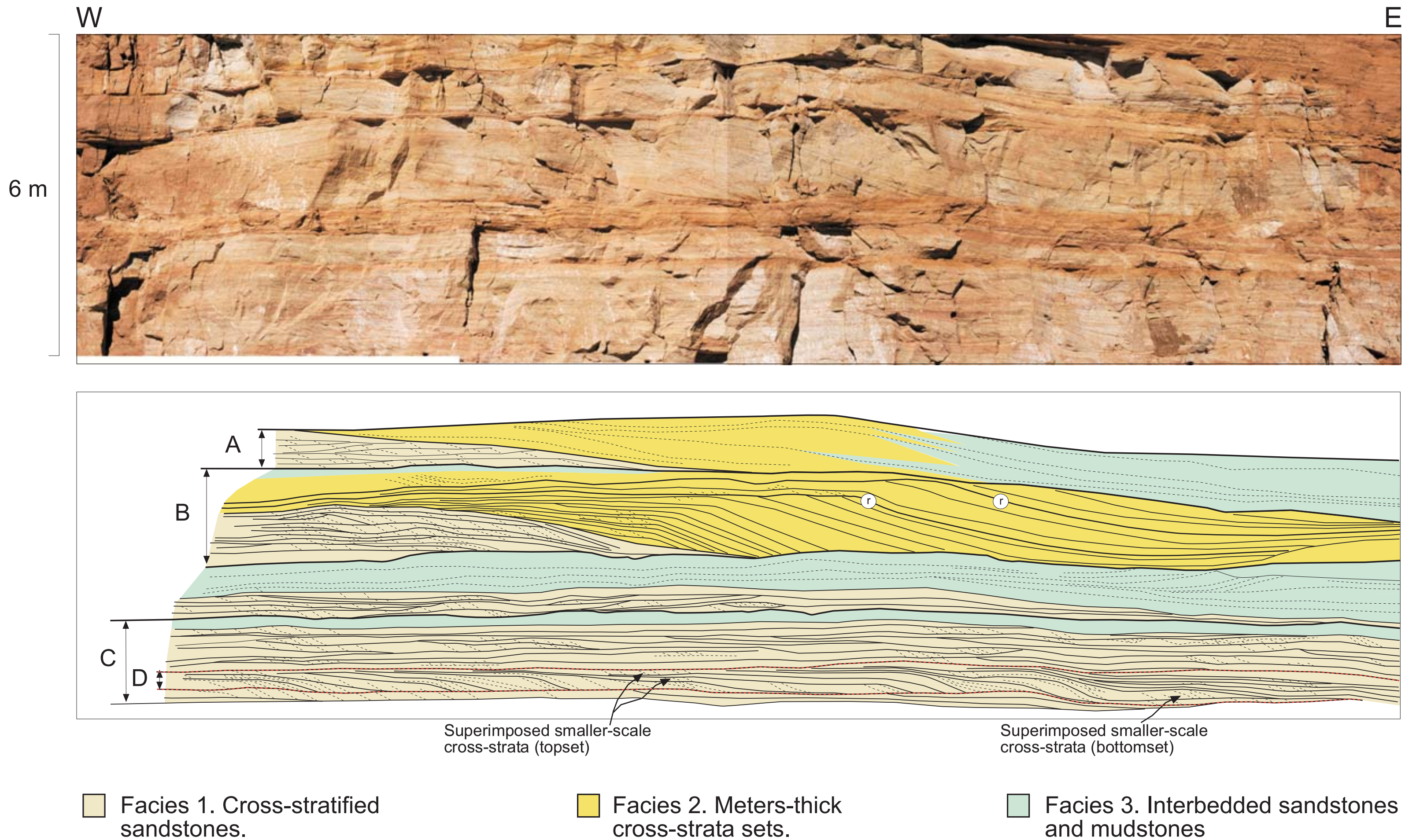

Fig. 12. Detailed bedding diagram. A) Lateral superposition of bedset type B and C. B) Lateral transition from facies 1 to facies 2. Note erosive horizontal topsets, and superimposed small-scale cross-stratification. The circled “r” denotes reactivation surfaces. C) Cosets of cross-stratification (facies 1). D) Example of sigmoidal cross-stratification with erosional topset strata and superimposed small-scale cross-strata. See Figure 8 for location (lower case c).

Reactivation surfaces can be defined by truncations of cross strata with differing inclination within a set. Less commonly cross strata graded gradually downcurrent into medium to fine grained, biotite-rich, massive to small-scale cross-bedded sandstone (Fig. 10B). Such fine-grained sandstones are recognized more commonly in cores than in outcrop. Decimeter-thick intervals of very coarse, chaotic or crudely cross-bedded sandstone can also be seen more commonly in core (Fig. 7) than outcrop (Fig. 10). Thin mud layers, 1 to 5 cm thick, also occur as laterally discontinuous layers that taper gently and gradually pinch out (Fig. 7, 10 and 11).

Interpretation

Cross-stratified sandstone formed by the migration of dune fields. Uniform dip directions within sets indicate dunes were formed mainly under unidirectional flow to the southeast. Local cross sets dipping toward the north record subordinate reversal of flows and may reflect the influence of tidal currents along mutually evasive paths. Individual cross-strata record avalanching of grains down the steep lee dune face followed by a period of grain fallout from suspension.

Sandier planar cross strata with high-angle dips relative to the basal erosion surface of a set, record dunes with strong lee flow separation and dominantly bedload sediment transport. Muddier concave-upward and sigmoidal cross-strata record increased suspension fallout rather than bedload transport, which suppressed the upward directed turbulence on the dune lee face. Where strata dip significantly less than the angle of repose, suspended sediment concentrations were high enough to suppress turbulence in the lee side of the dune and, therefore, a well-developed flow separation did not form (Mazumder 2003).

Cross strata with consistent dip along a set indicate that dunes migrated under fairly steady-state flow conditions (Roe 1987). Lateral transitions along a set from planar to concave-upward or sigmoidal cross-strata records progressive change in proportion of deposition from grain flow avalanches and suspension fallout. Such transitions likely reflect a progressive decrease in flow strength over time, or lateral flow deceleration and consequent increase in local suspended to bedload transport. The common occurrence of transitions from planar to lower-angle, upward-concave, cross-strata along sets suggests flow velocity fluctuation during deposition. Angle of repose cross-strata records the initial bedform build up to full lee vortex separation stage and relatively rapid migration of the dune as the lee face accretes by avalanches. Muddier concave-upward strata represent subsequent gradual dune abandonment, either because sediment transport shifts laterally or, more likely, as water discharge declines. Medium to fine grain-sized, biotite-rich, massive to small-scale cross-bedded sandstones, observed in the terminal downcurrent end of some individual cross-sets, formed under thick suspension clouds in the lee side of the bedform (Bhattacharaya and Chakraborty 2000).

Sigmoidal cross strata reflect faster vertical aggradation on the bed relative to rates of downstream dune migration, restricting erosion of the stoss side of the dune and thus allowing preservation of dune topsets (Chakraborty and Bose 1992). When sigmoidal cross-stratification is preserved, horizontal to low-angle inclined planar topset strata suggest high flow velocities, whereas smaller-scale ripple cross strata suggest vertical aggradation as flows waned. Preservation of sigmoidal cross strata may be favored in areas of flow expansion; for example, where dunes migrate into areas with slower flow or deeper waters.

Reactivation surfaces within cross sets reflect temporary filling of dune troughs followed by erosion, which probably record flow deceleration during depositional pauses, followed by trough erosion during a subsequent depositional event as discharge increases and lee flow separation intensifies. Such variations can reflect minor velocity variations associated with unsteady patterns of turbulence to the lee of the dune (Roe 1987), or longer term flow fluctuations related to tides or river floods. Small-scale cross-strata superimposed in the topset, or toeset of cross-strata, suggest smaller-scale dunes formed during shallow flows or ripples formed as flows slowed. Mud drapes within cross-sets also indicate episodic pauses in the migration of dunes that remained stable over multiple depositional events. Some massive sandstones rarely observed locally within cross sets may reflect slumping or liquefaction (Wilson 2001). Reactivation surfaces and discontinous mud drapes generally record shorter-term flow unsteadiness than that recorded by lateral changes in the character of strata along cross sets. Although such features can form due to large-scale patterns of turbulence within rivers, they tend to be much more abundant in tide-influenced deposits.

Facies 2. Meters-Thick Cross-Strata Sets

Description

Facies 2 consist of medium- to very-coarse grained sandstone occurring 1 to 2.5 meter thick cross sets (Fig. 9B). Their internal characteristics are similar to those of the decimeter-thick cross-sets of Facies 1, but they are distinctly thicker and more laterally extensive. Cross-strata can be planar, concave-upward or sigmoidal, and sets can contain internal reactivation surfaces and mud drapes. Planar cross-strata show dip angles as high as 22°, which, considering compaction, is at the angle of repose. Like the smaller scale examples they can display lateral changes in cross strata dip, grain size and the abundance of mud drapes. In some cases a co-set of smaller scale Facies 1 cross sets will pass gradually into a single large-scale Facies 2 cross set (Fig. 12B). Near these transitions, Facies 1 cross set bounding surfaces will dip systematically downstream, and locally Facies 1 cross strata occur within the larger-scale cross strata. In other cases significant increases in the amount of mud drapes along bottomsets of these larger-scale cross sets herald a lateral grading into mud-rich intervals of Facies 3 or 4 (Fig. 12A).

Interpretation

Depositional processes recorded by Facies 2 are interpreted to be broadly similar to those described above for Facies 1. These large cross sets are, however, distinct in scale; beyond the continuum of sizes of cross sets observed within Facies 1. Given that the thickness of dune cross strata sets broadly reflects water depths under which they form, an interpretation that these larger-scale cross sets also record migration of dunes would imply huge variations in flow depth relative to those in which the smaller cross sets formed. Gradual lateral transitions between co-sets of Facies 1 and these larger cross sets, and a lack of evidence for any erosion in these deposits on the order of five times the thickness of the large cross sets, do not support this interpretation. Rather these cross sets are interpreted to be the product of larger-scale bedforms, similar to alternate bars with steeply-dipping, lee Facies observed in some relatively straight river channels or larger-scale bars or “sandwaves” observed in some tidal systems. This interpretation is developed further in the subsequent sections that address Facies associations and bedding architecture.

Facies 3. Interbedded Sandstones and Mudstones

Description

This Facies consists of fine- to medium-grained, poorly-sorted sandstones interbedded with mudstones of Facies 4 (Fig. 9C). Sandstone and mudstones alternate vertically over a few centimeters- to decimeter-thick, defining broadly horizontal beds that are continuous over several to tens of meters, normally more laterally continuous in exposures parallel to paleoflow directions. The base of a sandstone bed abruptly overlies an underlying mudstone, whereas the sandstone commonly grades upward to the overlying mudstone. Although thin cross-strata sets can occur at the bottom of a sandstone bed, these deposits are more typically very fine-grained, rippled sandstones. Mudstones are mostly composed by massive or laminated silt. Sometimes biotite-rich sand laminae are observed within the mudstones. Successive beds can have fining- and thinning-upward trends, in which the sandstone proportion tends to decrease (Fig. 9C). Small synsedimentary deformation structures occur within this Facies when observed in core (Fig. 7). Bioturbation can be observed within the mudstone beds and it increases in abundance upward within these bedding successions.

Interpretation

These fine-grained rocks reflect low energy suspension sedimentation and weak traction current activity. The complex interbedding of sandstones and mudstones are the result of frequent, rapid alternation of current strength. Cross-bedded sandstones grading vertically to horizontally laminated mudstones, record a gradual decrease in flow strength, suggesting that each depositional sandstone —mudstone bed was formed during a single flood event. Bedload transportation was probably the dominant mechanism during sandstones sedimentation, forming the cross-bedded and rippled units. Mudstone intervals were deposited by suspension, under lower flow strength conditions. Stacked interbeds with a fining-upward trend probably represent a progressive decrease in flow velocity over successive flood events. Soft-sediment deformation observed in core attests to intermittent rapid deposition of sand upon mud and associated rapid dewatering.

Facies 4. Isolated Mudstones

Description

Facies 4 is structureless to horizontally laminated, silty to sandy mudstones (Fig. 9D). This Facies appears as an isolated decimeter-thick mudstone layer that commonly can be traced as a distinct bed over tens of meters, rather than interbedded with sandstone beds as in Facies 3. Although this is the only Facies that is commonly bioturbated, rare bioturbation is also observed in thin mudstone drapes within sandstone-dominated Facies. Trace fossils can be rich enough in this Facies that they can be seen along the base of bedding planes from a safe distance from the quarry wall. Traces within other Facies were observed on displaced blocks along the quarry floor. Smooth-walled vertical to sub-vertical traces are loosely classed as *Skolithos* (Fig. 13A). Simple meandering burrows oriented horizontal to bedding are classified as *Planolites* (Fig. 13B and C). Bedding-plane resting and crawling traces on exposed sandstone-mudstone contacts are associated with *Rusophycus* and *Cruziana* respectively (Fig. 13D and E).

Interpretation

These low energy suspension deposits suggest relatively long periods of slow deposition. These layers may record large-scale shifts in deposition. Burrowing animals first appear near the end of the Neoproterozoic and the abundance and depth of bioturbation increased in a stepwise manner through the Phanerozoic (Macnaughton et al. 1997). Neoproterozoic trace fossils are typically horizontal, unbranched trails or burrows made close to the sediment surface. Although in the Cambrian animals probed deeper into the sediment and produced more complex burrows (including branching forms and concomitant expansion in the range of sizes; Jensen 2003), the variety and range of ichofabrics remain restricted. Miller (1984) observed that aquatic terrestrial sediments were not colonized by burrowers before the beginning of the Permo-Triassic. Trace fossils in older strata thus appear to be exclusively in marine sediments (Amireh et al. 1994).

Cruziana is interpreted to be a locomotion trace made by a trilobite or trilobite-like animal as it crawled along the sediment surface, and *Rusophycus* is related to the resting trace of trilobites. *Skolithos* and *Planolites* are typical of shoreline environments but are also common farther seaward in shallow shelf environments (Boggs 2001). *Cruziana*

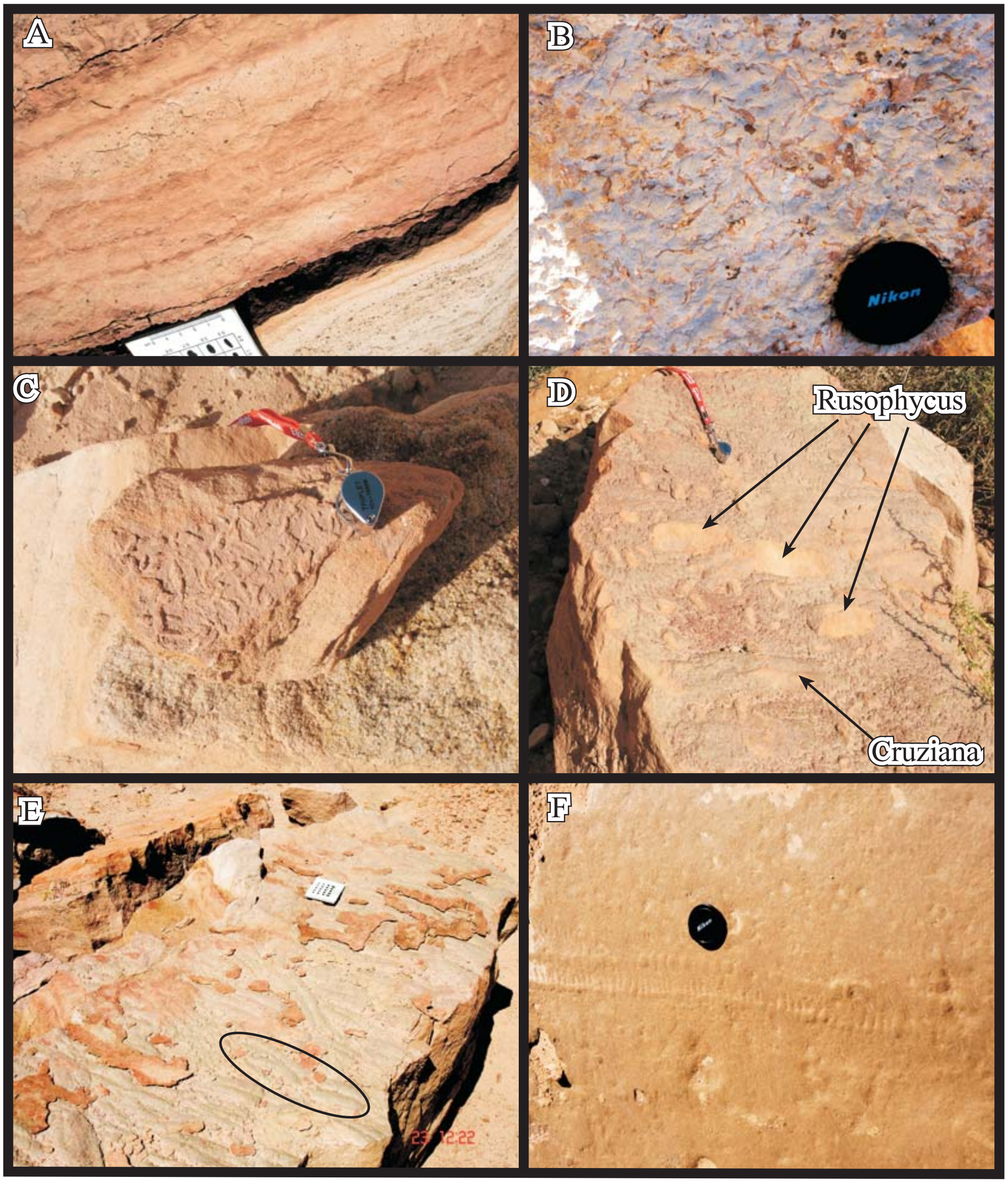

Fig. 13. Representative photographs of bioturbation. A) Skolithos. B) Planolites. C) Planolites. D) Cruziana. E) Rusophycus. F) Cruziana.

and *Rusophycus* tend to form in deeper waters, but they can also be present in sediments from some nearshore environments. Therefore, bioturbation within the mudstone Facies suggest a shallow marine environment temporary inhabited by animals (Haddox and Dott 1990).

Bioturbation within the Hickory Sandstone has been recognized by previous workers. Barnes and Bell (1977) assigned bioturbation to the *Cruziana* ichnoFacies. Cornish (1975) described several ichnofossils, including trilobite crawling traces, resting traces, and scratch marks. He also found *Diplocraterion* and *Planolites* in abundance. Krause (1996) identified U-shaped burrows classified as *Diplocraterion* and evidence of trilobite crawling traces and feeding structures on bedding surfaces within his burrowed lithoFacies. Wilson (2001) recognized *Planolites* or possibly the meandering burrow of *Cosmorhaphe*, and more rarely *Diplocraterion*, *Cruziana* and *Skolithos*.

Correlation of Facies with Previous Studies of the Hickory Sandstone

Facies described in this study are equivalent to the upper interval of cross-bedded lithoFacies (subFacies HXc) defined by Krause (1996), characterized by unidirectional cross-bedded sandstones, significant bioturbation by marine organisms, and the first appearance of tidal-influenced deposits. Krause (1996) interpreted this subfacies to record the beginning at the transition between the underlying terrestrial fluvial and alluvial Facies and the overlaying marine-influenced Facies of the upper Hickory. Wilson's (2001) cross-bedded subFacies XB2 are also comparable with the deposit analyzed in this study and consists mainly of trough cross-bedded sandstones with bioturbation and fine sediments increasing upward. Wilson (2001) also interpreted this subfacies as the transition from basal fluvial deposits into a fluvial-influenced, intertidal sand flats to subtidal inner estuarine deposits.

FACIES VARIATIONS WITHIN BEDSETS

Bedsets are defined by systematic vertical and lateral changes in Facies. All bedsets, several decimeters to a few meters thick, have broadly sheet like geometry. Bedsets generally continue laterally from many tens to hundreds of meters, but not for the entire half-kilometer exposed in quarry walls. They are delineated by an erosional base, are generally dominated by sandstone Facies, and are capped by muddier intervals of Facies 3 and 4 or by the erosive base of the bedset above. Lateral Facies assemblages within bedsets comprise a group of genetically related strata. Four typical types are described and interpreted below in order to present the range of variability (Fig. 6). Specific bedsets may fall between the end member types.

Bedset Type A

Description

Bedset A is dominantly cosets of Facies 1 (Fig. 6A) and has tabular, or rarely concave-upward shape (Fig. 14A1). The erosion surface at the base of a bedset is normally horizontal, but can be more irregular where local scours cut centimeters to a decimenter into underlying deposits. Bedsets can either be laterally continuous across the hundreds of meters exposed in the outcrop or can terminate where an overlying bedset thickens and erodes deeper, or can grade laterally into other Facies defining other types of bedsets. Although cross-set bounding surfaces within bedsets are generally parallel with the basal erosion surface, in some cases they downlap the basal erosion surface at low angles (less than 6°) (Fig. 10A). Such systematic dip of cross set bounding surfaces defines the geometry of beds within these bedsets. In most cases bed

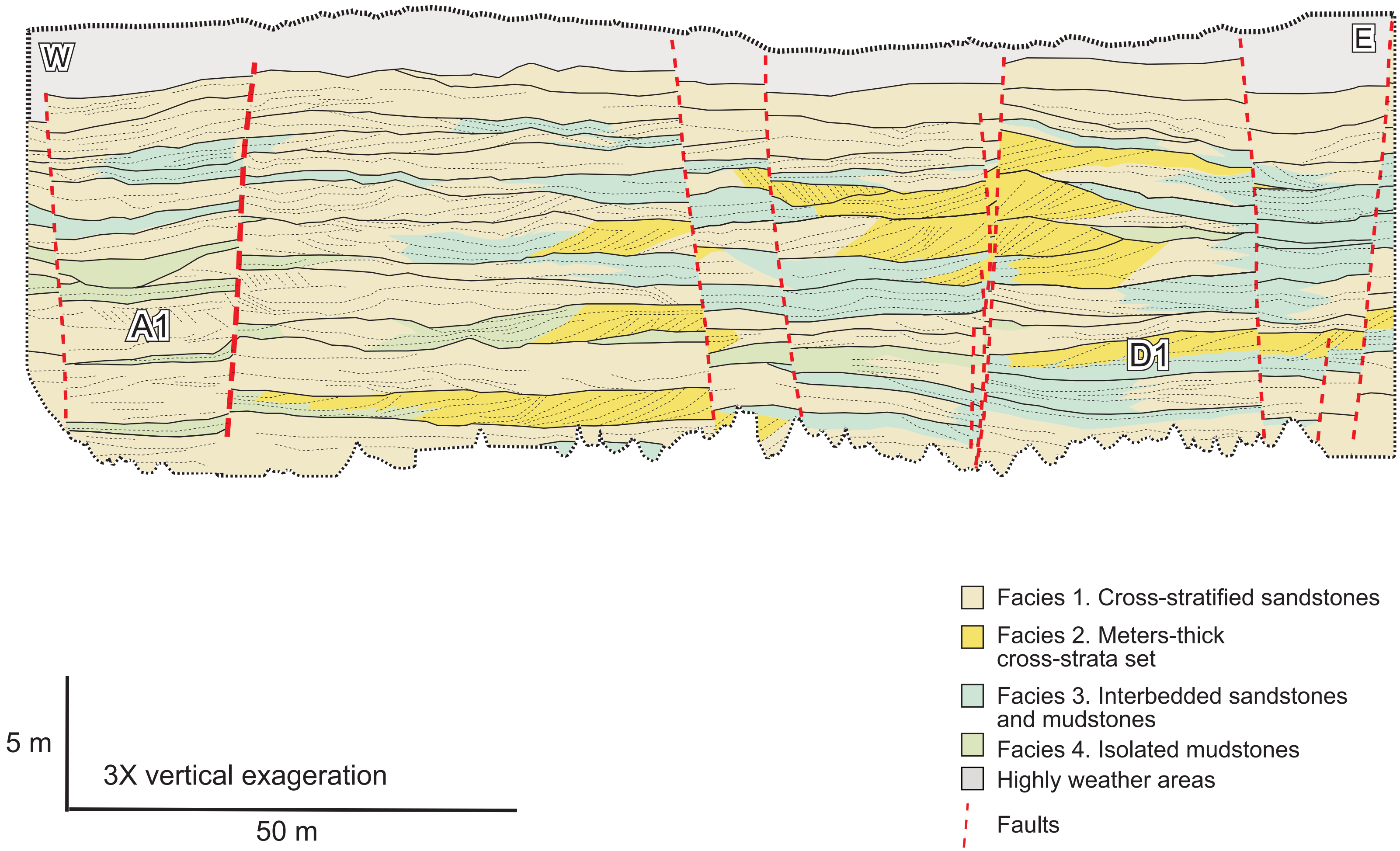

Fig. 14. Bedding diagram of HIC03 showing examples of bedset types A (A1 in the diagram) and D (D1).

to set basal erosion surface downlap relationships are quite subtle and difficult to recognize due to varying depth of incision along the base of individual cross sets. Bedding surfaces normally dip in about the same direction as internal cross-strata. In a few locations, bedding surfaces change in dip direction along the bedset, defining broadly convex-upward beds (Fig. 15A2).

Although grain size and cross set thickness decrease slightly upward within bedsets (Fig. 11C), this trend is normally subtle due to stronger grain sorting within individual cross strata sets. Basal deposits within a bedset are generally coarse to very coarse-grained, whereas high in a bedset deposits tend to be medium to fine grained. Bedsets can be capped by massive or small-scale cross-bedded sandstone, or a millimeter to centimeter-thick rippled to horizontally laminated, laterally discontinuous, sandy or silty mudstone layer of Facies 4 (Fig. 11). Massive sandstone deposits locally capping bedsets are generally quite thin and are thus easier to recognize in core than in outcrop. In many cases, however, the sand sheet has been eroded by the basal erosion surface of the bedset above.

Interpretation

The tabular geometry and dominance of Facies 1 suggest deposition of a field of dunes. The basal erosion surface and internal inclined beds suggest the dunes were migrating across a larger-scale barform, which had low-angle faces. Where the bedset has a concave upward base, the bar may have been migrating within a shallow channel. The bedset thickness is assumed to scale to about 80% of flow depth. Thus, whether formed in channels or broader, less-restricted areas of flow, water depths were at most a

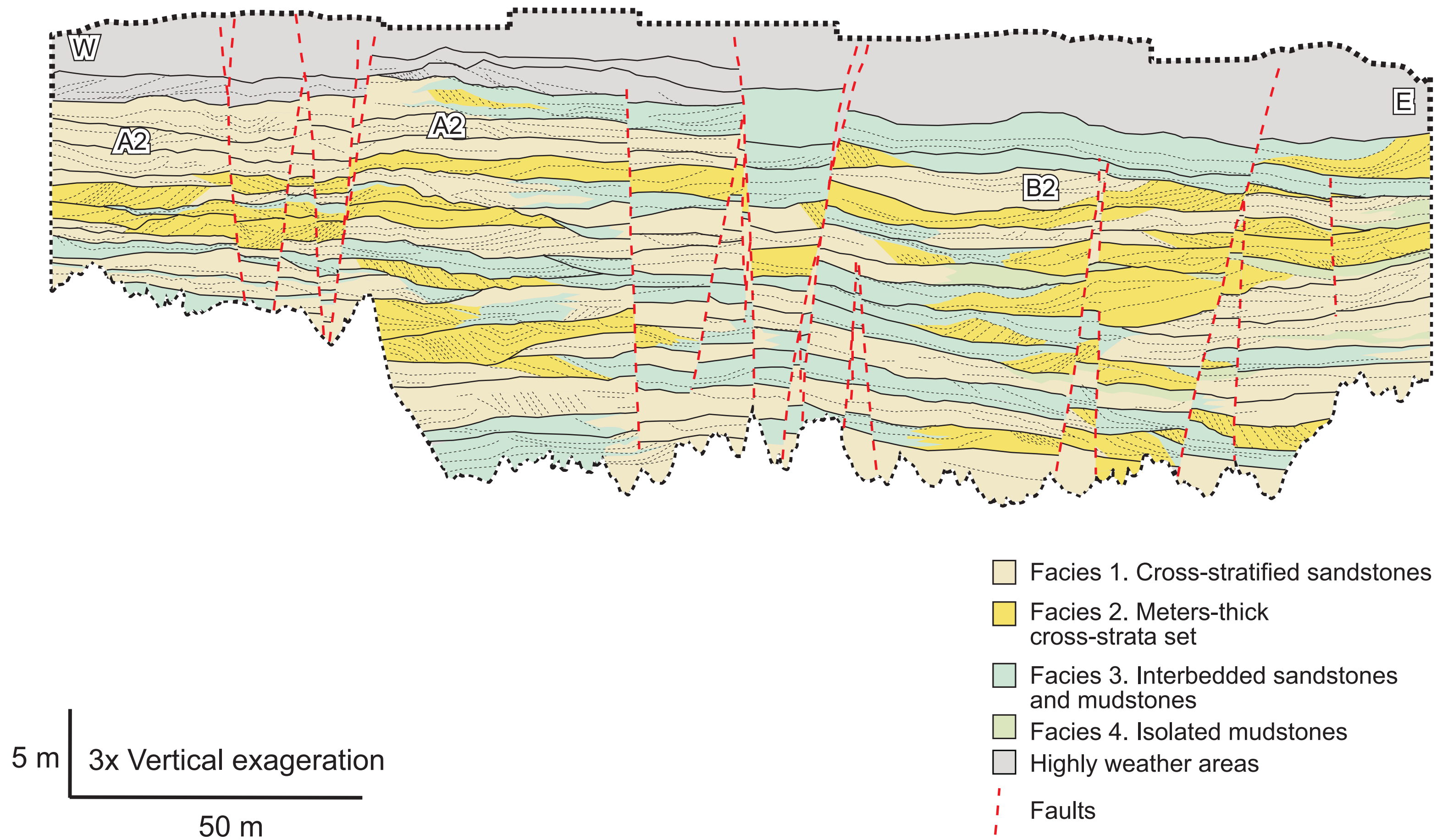

Fig. 15. Bedding diagram of HIC07 showing examples of bedset types A (A2 in the diagram) and B (B2).

few meters deep (Willis 1997). Lateral continuity of bedsets perpendicular to paleoflow suggests bars (and associated channels) were at least several tens of meters wide and possible up to several hundred meters. Miall (1985) proposed that in channels with high width/depth ratios, dips of the accretion surfaces can be very gentle. Reversal of bed dip direction along some bedsets reflects lateral accretion on both sides of a bar deposited in the middle of a channel. This is indicative of braided-patterns rather than undivided channels.

Vertical changes in cross-set thickness upward within individual cosets record decreasing dune size toward the bar top, as dunes scale to flow depth (Best et al. 2003). Laterally discontinuous mud drapes are interpreted as low stage, fine-grained drapes deposited on top of the bar. Mostly uniform paleocurrent patterns observed in the medium- to small-scale cross-stratification and the cross-set bounding surfaces support domination of unidirectional flows during deposition. This paleocurrent pattern, together with the angle of repose cross-strata described in Facies 1 suggests the channels had significant fluvial influence. However, predominance of cross-strata with concave-upward internal shape and sparse dipping-opposite cross-stratification are probably indicative of at least minor marine influence during deposition.

Bedset Type B

Description

Bedset changes downstream from a cross-stratified coset of Facies 1 to a single, large cross set of Facies 2 (Fig. 6B1) or vice versa (Fig. 6B2). This sheet-sandstone bedset show thicknesses not greater than 2.5 meters and, in some cases, the thickness can vary along the transition.

Downstream transition from low-angle-dipping beds within cosets (Facies 1) to thinner, more steeply dipping cross-strata (Facies 2) can be gradual (Fig. 16B1) or can occur across a low-angle inclined erosion surface that separates the two components (Fig 12A, B). On the other hand, lateral transition from a set of thick cross-strata (Facies 2) to the cosets defined as Facies 1 occurs gradually as the large-scale cross-strata progressively decline in dip and become gently dipping surfaces, bounding medium- and small-scale cross-stratification sets (Fig. 6B2).

Interpretation

Bedset B is interpreted as the interaction between broad gentle bars and angle-of-repose bars. Transitions from low-angle-dipping beds within a thicker coset to a single thick cross set within these bedsets are interpreted to record the development of flow separation at the downstream end of a bar. The initial deposits record continuous migration of dunes across the sediment bed. As the bar builds upward it restricts flow, which expands past the bar crest and decreases in velocity enough to produce flow separation. Once flow separation develops, migrating dunes tend to collapse at the downstream edge of the bar crest rather than migrating continuously downstream. As the zone of flow separation strengthens, the front of the bar may develop into an angle of repose dipping face. Bedsets with gradual transitions probably record a period when flow separation past a bar only developed during high flows, and dunes still migrated past the bar crest during lower stages of flow. Erosional transitions along a bedset may

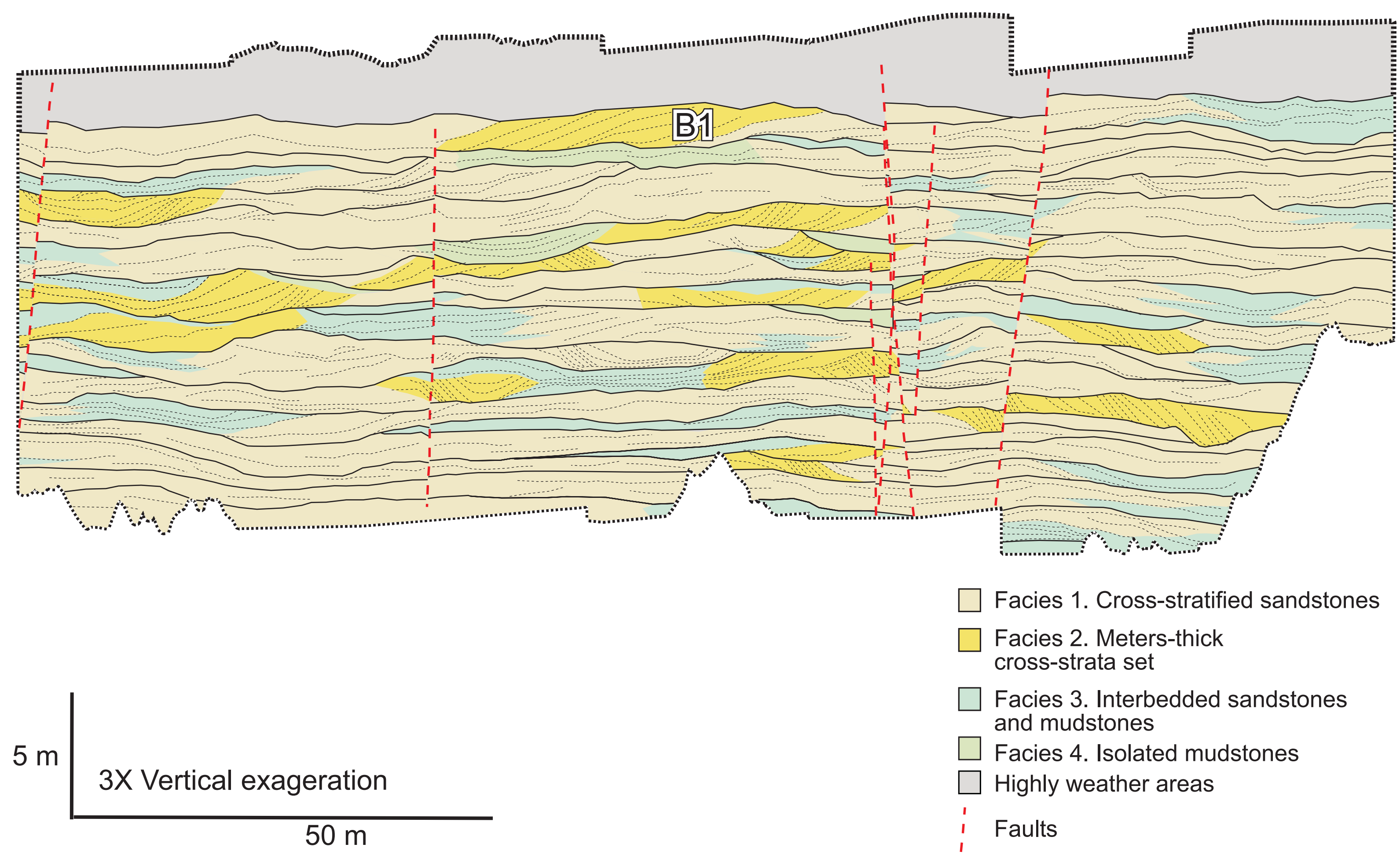

Fig. 16. Bedding diagram of HIC04 showing an example of bedset type B (B1 in the diagram).

record erosion of the front bar face during rising flow stages as the zone of flow separation strengthened.

In contrast, transition from large solitary sets to cosets of cross-stratification suggests a decline in velocity possibly associated with lowered discharges (Roe and Hermansen 1993). The solitary large-scale cross-stratified sandstone probably records the growth of angle-of-repose bars and subsequent migration. Sandstone beds with cosets, found downcurrent, records the migration of dunes down the front face of the sand body and the flattening out of lee faces on the migrating bars as migration rates of the bedform slowed due to weakening currents (Willis et al. 1999).

Bedset Type C

Description

Bedset C contains lateral gradation from solitary large sets of cross-strata (Fig. 6C1) or cosets of cross-stratification (Fig. 6C2) to mudstone-rich deposit of Facies 3 or 4. Although broadly tabular, this type of bedset can significantly thin and then terminate at a steeper concave-upward margin where it fines into mudstone (Fig. 17C1). Within an individual bedset, thicknesses along mudstone intervals are generally thinner than those where sandstone deposits dominate. The common lateral extension of Facies 2 within this element is a few tens of meters, but distances as long as 90 meters can be seen.

When Facies 2 grades laterally into mudstone-rich deposits, large-scale cross-sets display a progressive decrease in dip-angle and a progressive lateral trends in abundance of mud drapes that terminates with horizontally interbedded mudstones and sandstones of Facies 3 (Fig. 12A), or with homogeneous mudstone of Facies 4 (Fig. 18C2).

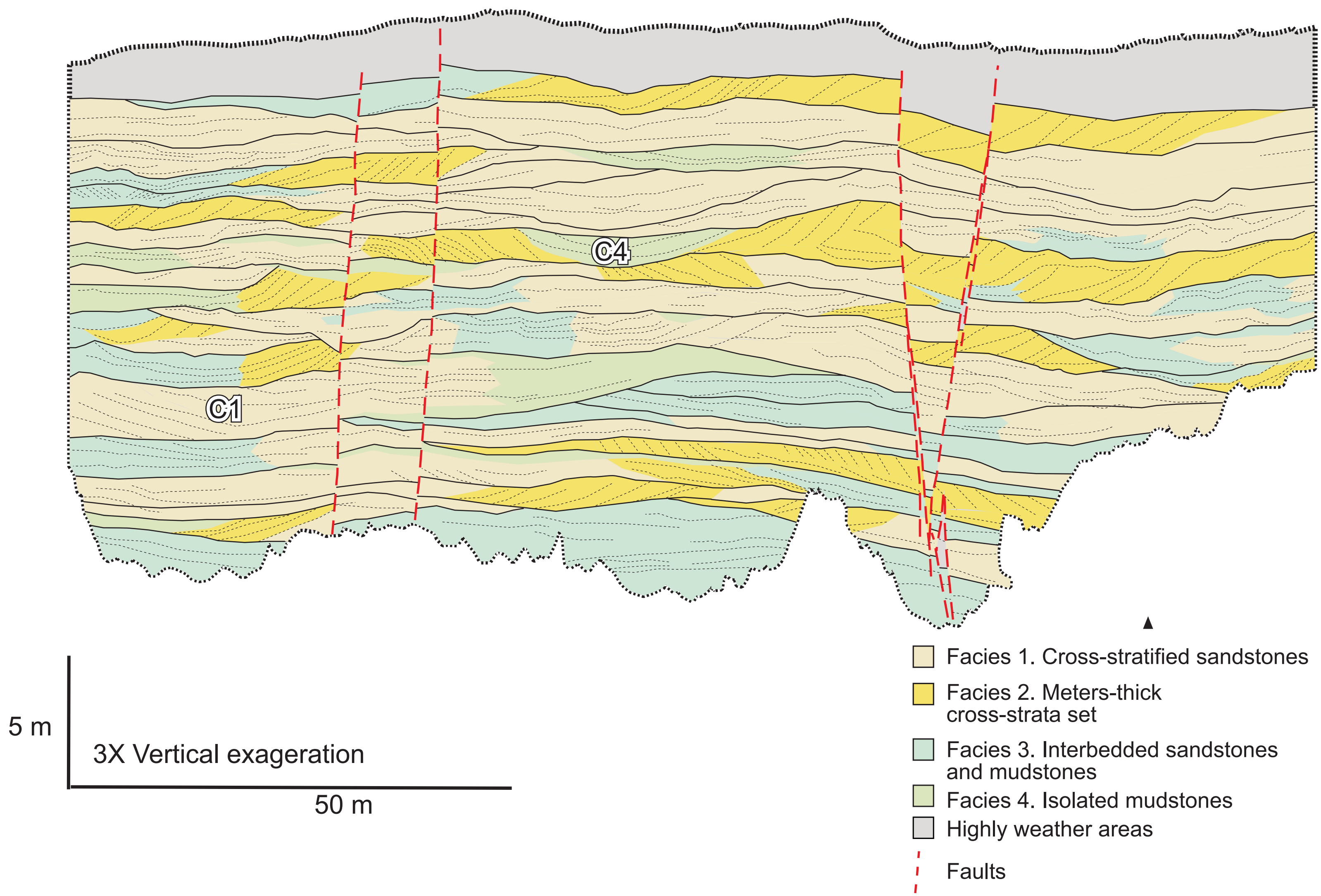

Fig. 17. Bedding diagram of HIC01 showing examples of bedset type C (C1 and C4 in the diagram).

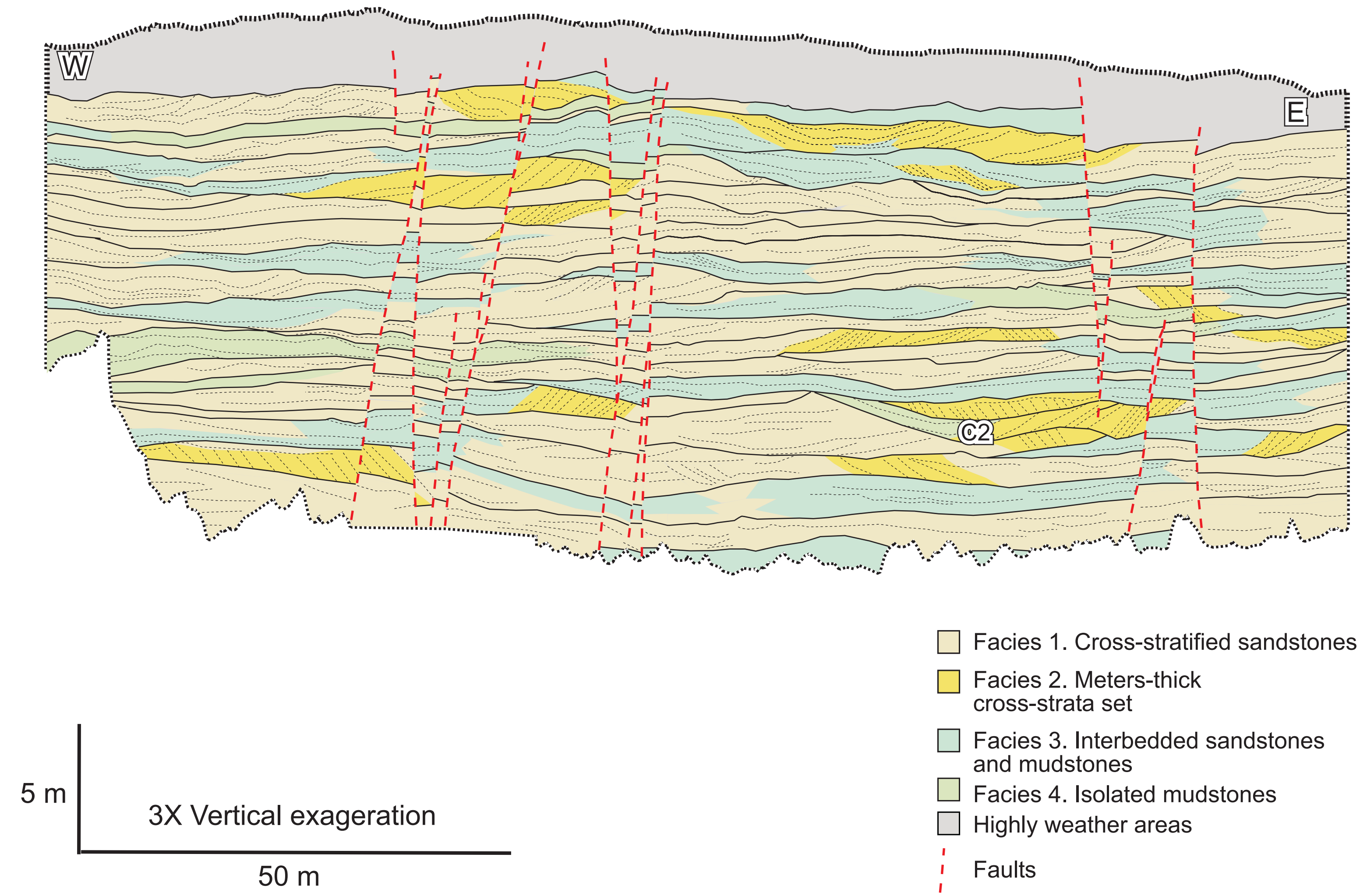

Fig. 18. Bedding diagram of HIC02 showing an example of bedset type C (C2 in the diagram).

At the transition from Facies 1 to 3 cross strata contain discontinuous internal mudstone drapes (Fig. 6C2). In some locations, these mud drapes are capping cross-bedded cosets that shows a vertical decrease in cross-set thickness. A few centimeters to decimeters mudstone commonly caps the bedset.

In most cases, beds within sets dip in the same direction from one margin of the bedset to the other. In some cases, however, sandstone beds dip in both directions away from the center of a bedset, and successive beds show opposite trends in grain size fining toward their respective margins. The final result is sandstone Facies with internal convex-upward beds dipping towards both margins, some of them downlapping on the erosional base, and some of them grading laterally to horizontally stratified toeset deposits of Facies 3 or 4 (Fig. 19C3). In a few cases, sandstone beds dip from both margins toward the centre of the bedset. In these latter cases the deposits separating beds with opposite directions of dip are commonly muddy (Fig. 17C4).

Interpretation

Bedset records accretion of a bar and an adjacent channel fill. The concave upward shape of the bedset bounding surface is probably indicative of lateral channel migration. Thinner mudstone intervals are probably the result of differential compaction. Bars of Facies 2 with lateral extent no longer than few tens of meters are probably indicative of low sinuosity channels that migrated little before channel switching and abandonment. Transitions from sandstones to mudstones record gradual reduction in discharge over several flood events and subsequent channel abandonment. Where a bedset ends in horizontally bedded mudstones of Facies 4, more rapid abandonment of the channel is

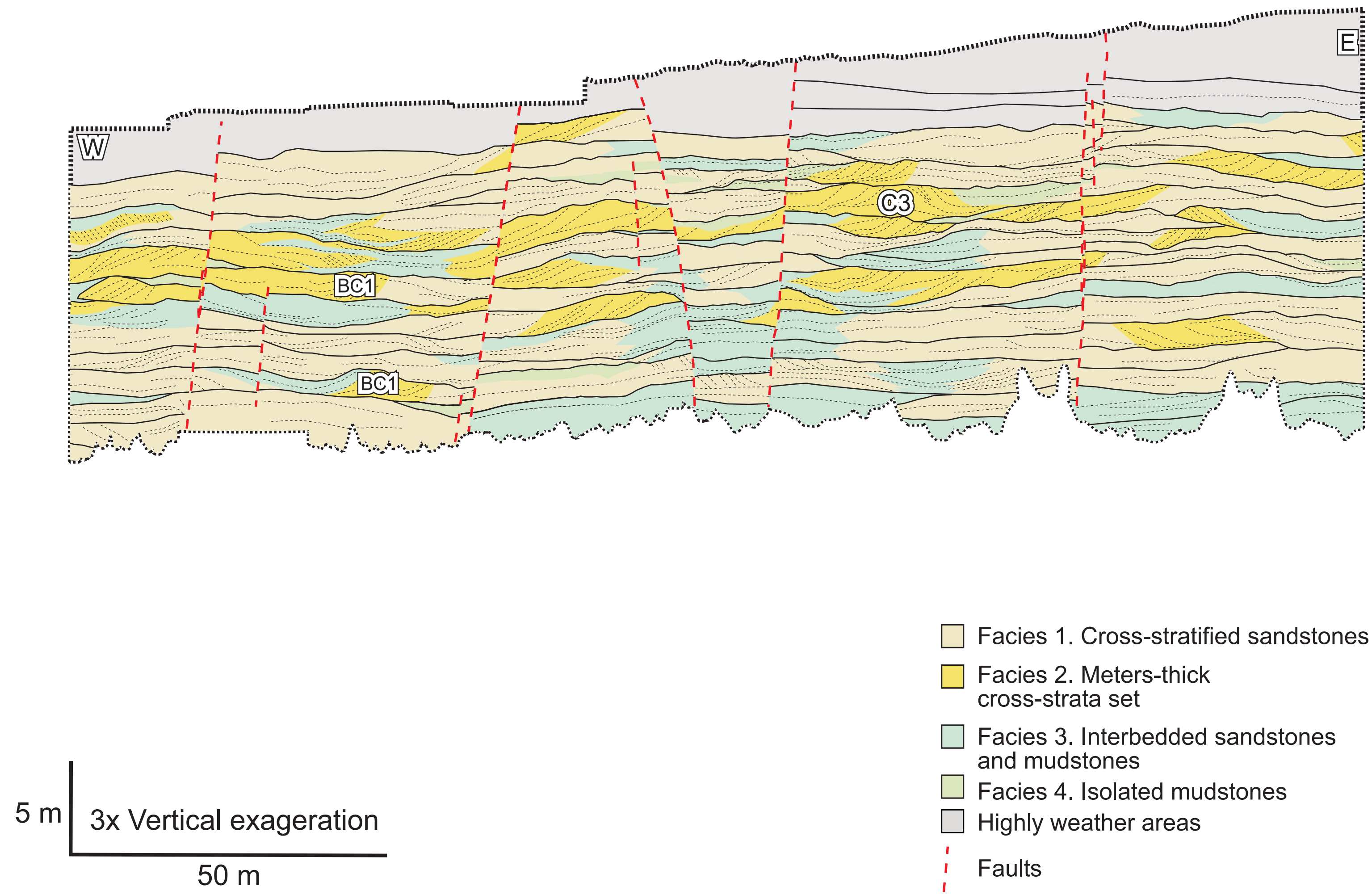

Fig. 19. Bedding diagram of the central portion of HIC08/HIC09 showing examples of bedset type C (C3 in the diagram) and superposition of bedset types (BC1 in diagram).

suggested. Bed dip and Facies trends along a bedset are indicative of deposition within braided channels. Convex-up beds can be interpreted in terms of cross sections of a mid-channel bar exposed in an outcrop perpendicular or highly oblique to the paleocurrent direction (Allen 1983).

Bedset Type D

Description

Bedset is defined by a solitary large-scale cross-set of Facies 2 that grades laterally directly into mudstone Facies (Fig. 6D). The sandier segment of the bedset is underlain by a basal erosion surface, but the base of the muddier part appears conformable with underlying deposits. Although the transition of Facies 2 into mudstone Facies is broadly similar to that described for bedset type C (above), in this case the mudstone Facies interfinger vertically with the sandstone cross strata rather than reflecting a progressive change across subsequent beds along the set (Fig. 14D1).

Interpretation

Interfingering of sandy cross strata with mudstone suggests abrupt alternation in flow speed through time. Lateral change from sandstone to mudstone along the bedset suggests rapid lateral decline in average flow rates down dip. These variations are interpreted to record mouth-bar deposits formed at the end of distributary channels. The transition from confined to unconfined flow at the end of these channels produces a decrease in velocity, and the sedimentation of mouth-bars, depositing the coarser-grained sands of Facies 2 in the immediate vicinity of the river mouth and finer-grained sediments (Facies 3) in areas seaward of the river mouth (Coleman 1980). The lack of erosional surfaces within the bedset suggests that these bars are not migrating over a confluence scour zone, as has been proposed for deposition under confined flow conditions within a channel (Bridge 1993a), but at the mouth of distributary channels, where flow expansion causes deceleration and mostly sedimentation without any erosive surface at the base. Where the vertically-stacked elements are dipping in the same direction, they record mouth-bar deposits formed by different flooding events. The whole sequence records the progradation and retreat of mouth bars through time.

Superposition of Bedsets

Description

Within a single interval, bedsets can be overlapped creating a complex alternation of sandstone and mudstone deposits. This superposition is characterized by bedset types A, B and C overlapping, forming a complete sequence of Facies 1 grading into Facies 2 (or vice versa) and finally into mudstone Facies 3 or 4 (Fig. 12A). This can occur within a concave-upward shape usually at one side of the bedset, where the mudstone Facies were deposited (Fig. 19BC1), or it can occur within a sheet-like bedset where this Facies assemblage normally shows a symmetric pattern (Fig. 20BC2). When this is the case, sandstone layers are dipping in opposite directions, toward the central mudstone interval.

Interpretation

Superposition of bedsets are the result of the initial formation and migration of a bar (bedset A, B) and the subsequent channel fill after channel abandonment (bedset C). When this bedset assemblage shows a symmetric pattern, lateral accretion of two bars converging at the same channel segment is inferred. This pattern is supportive of braided channels rather than undivided channels.

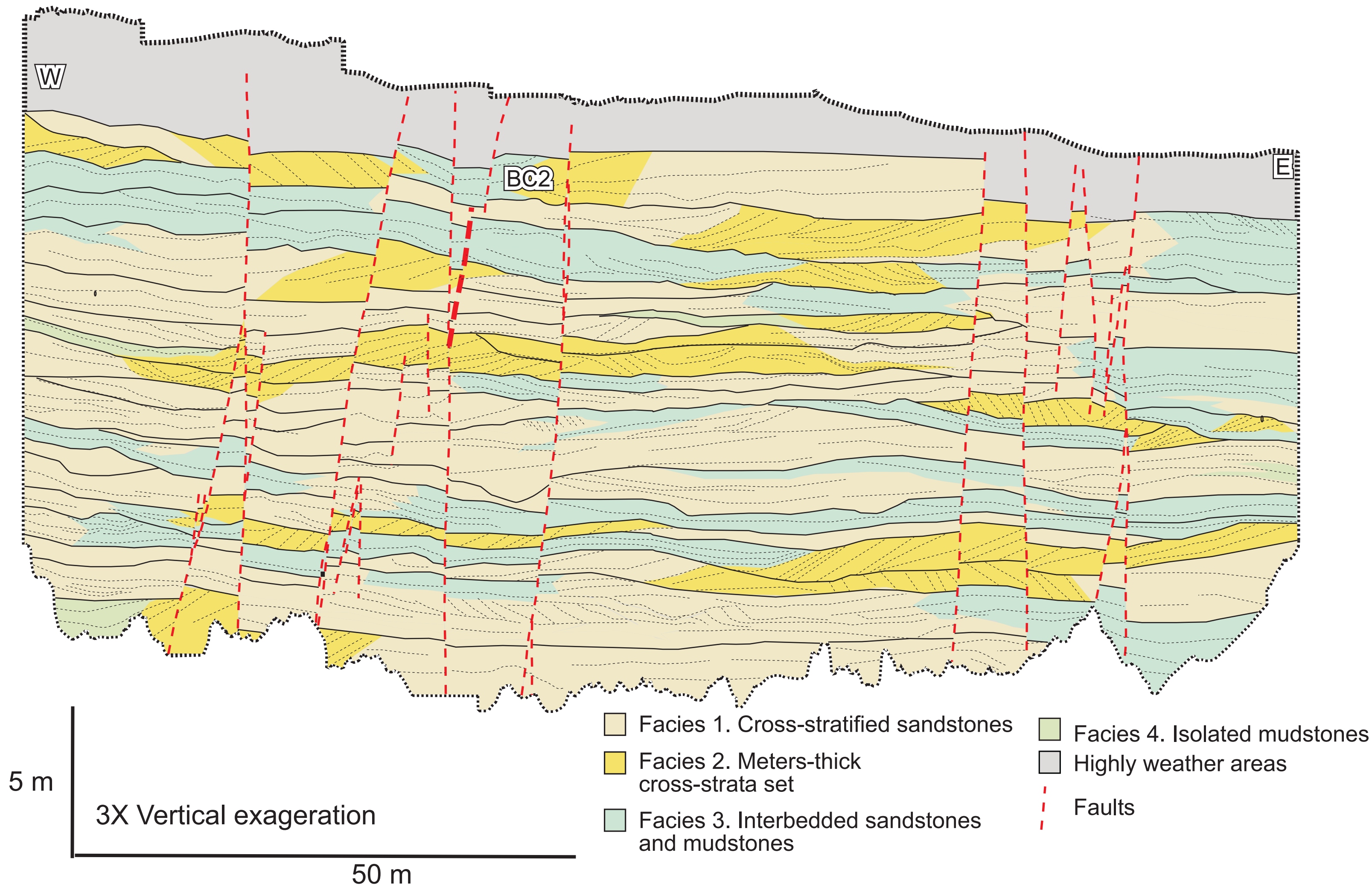

Fig. 20. Bedding diagram of HIC05 showing an example of symmetric superposition of bedsets (BC2 in the diagram).

BEDSET ARCHITECTURE

Bedsets are stacked in a fairly random pattern within the quarry exposures. Mudstone layers capping bedsets and locally thickening within channel fill deposits are commonly discontinuous along exposures. Although there is a subtle vertical increase in mudstone beds upsection, seen more clearly in core than the quarry exposures, in general the types and stacking of bedsets is fairly stationary. Similarly, no major erosion surfaces are recognized that might be used to define longer-term erosion events. Therefore the deposits lack clear vertical trends or cyclicity that could be used to define larger-scale hierarchy of depositional beds.

Despite the lack of obvious larger-scale allostratigraphic surfaces, variations of bedsets and their internal Facies could be compared between successive quarry walls (HIC03, HIC06 and HIC08) to define the three-dimensional depositional architecture. The architecture of bedsets along four intervals are defined and interrupted in terms of their genetic association (Fig. 21A). Sedimentary Facies within the focal intervals observed in multiple quarry exposures are labeled with letters on each cross section (Fig. 21A) and on the interpretive 3D reconstructions (Fig. 21B) to show correlations between the two diagrams.

Interval I

Deposits along this layer are relatively rich in mudstone (Fig. 21B). Transition from small-scale cross-stratified sandstones of Facies 1 (letter ***a*** in Fig. 21A) to solitary large sets of cross-strata of Facies 2 (***b***) is the result of lateral migration of a bar. Mudstone Facies 3 (***c***) was formed by filling of the associated channel segment after abandonment.

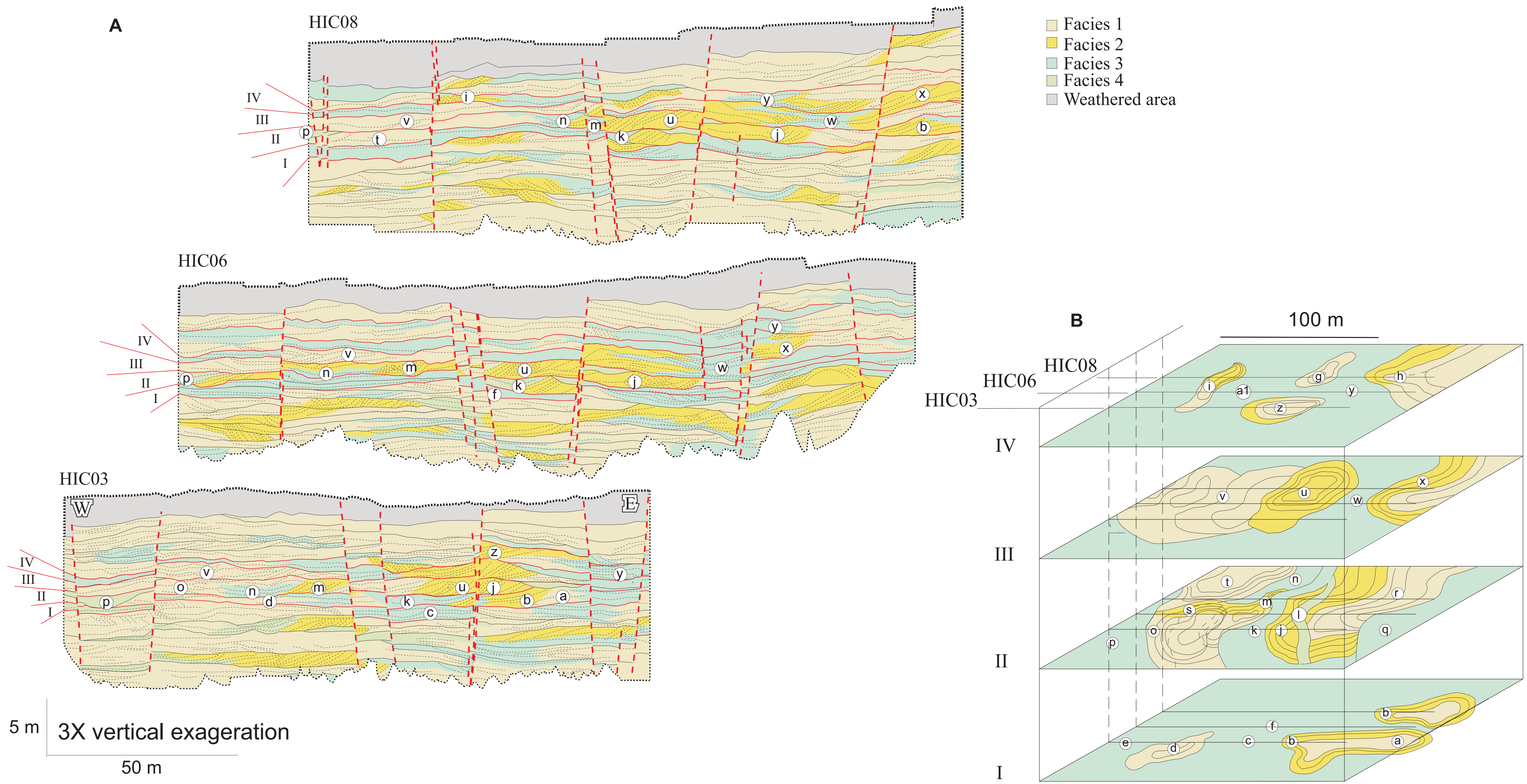

Fig. 21. Detailed 3D reconstruction. A) Bedding diagrams of quarry walls showing lateral variation of facies. Red lines represent bedding surfaces correlated in the three walls. See Figure 5 for location of the quarry walls. B) Schematic visualization of the intervals in 3D. Interval I is the older and IV the younger. Circled letters are use to correlate observation in quarry walls with the 3D interpretation.

Thinner sandstone deposits (labeled ***d***) are interpreted to be a smaller mid-stream bar separating channel filling deposits (***c***, ***e***). Sandy bedsets separated by muddier channel filling bedsets is consistent with deposits of bars within a braided river.

Interval II

Inclined beds labeled ***m*** in HIC06 (Fig. 21A) represent the sandier part of a bedset type D, interpreted to be a mouth-bar deposit. This bedset remains the same type where exposed in HIC03 (***m***). Mudstone deposits (***n***) exposed in HIC08 are interpreted to be formed by the associated distributary channel responsible for the mouth-bar deposition. Progressive lateral accretion of the mouth bars and filling of the distributary channel reduced flow velocity and sediment discharge, leading to channel abandonment. Facies 1 deposits labeled ***t*** are interpreted to be deposits of a broad gentle bar or vertical aggradation of channel floor. Superposition of ***r***, ***j*** and ***k,*** easily correlated between the three quarry walls, represent overlapping of bedset types A, B and C, which is indicative of lateral growth of a bar and filling of a channel after abandonment (Fig. 21A). The planar erosive surface with a gentle concave-upward geometry at the western tip of these overlapping bedsets, supports the interpretation that these deposits formed by lateral migration of a channel, eroding previous mouth bar deposits (***m***). The pronounced grain size contrast between laterally accreted bar and channel-filling deposits supports that there was an abrupt abandonment of the channel segment. Facies 4 labeled ***l*** comprise a small concave-upward shaped body located at the top of the bar (Fig. 21B) that can be correlated between the three quarry walls. It is probably related to a cross-bar channel fill.

Interval III

It is characterized by deposits of a channel fill separating channel bars (Fig. 21B). Large-scale cross strata of ***u*** (Fig. 21A) are dipping in opposite directions showing a convex-upward shape in quarry walls HIC06 and HIC08. This large-scale cross-stratified sandstone is superposed laterally with trough cross-bedded sandstones of Facies 1 to the west (***v***). This superposition of bar deposits (***u*** and ***v***) suggests that bars were coalesced by lateral superposition, forming a large bar complex. Dipping in the opposite direction, ***u*** grades laterally into heterolithic deposits of Facies 3 (***w***). In HIC06 and HIC08, ***w*** grades laterally to another set of Facies 2 (***x***). The lateral superposition of ***u***, ***w*** and ***x*** records two bars (***u***, ***x***) migrating laterally toward the channel segment (***w***).

Interval IV

Small isolated sandy bodies (***z***, ***i***, ***h***, ***g***) are separated by mudstones (Fig. 21B). Letter ***z*** is the sandier part of a typical example of the overlapping of bedset types A, B and C, which record bar accretion and channel-filling (Fig. 21A, HIC03). Sandstone ***i*** (Fig. 21B) is probably the result of accretion of a broad gentle bedform that had a steeper lee-faces toward the north (HIC08). Letter ***h*** is a typical bedset type D, interpreted to be a mouth-bar deposit. However, an erosive surface separating the vertically-superimposed bars suggests that ***h*** formed due to bar migration over a confluence scour zone, and is thus characteristic of deposition within channelized flows.

DISCUSSION

Evidence for rapidly fluctuating flow velocities, such as lateral variations of cross-strata shapes, mud drapes within cross-sets and superimposed small-scale cross-strata on larger-scale foresets, is ubiquitous in these deposits. Whether these flow velocity fluctuations are the result of flashy fluvial discharge or tidal influence is less clear. Although cross stratification within Facies 1 and Facies 2 generally all have the same dip direction, dominantly to the southeast, locally cross-strata with opposite dip directions are observed. Although tidal action is commonly inferred from the local occurrence of mud drapes, herringbone cross stratification, sigmoidal bedding, and reactivation surfaces, these features are not always diagnostic of tidal activity (Nio and Yang 1991). Mud drapes can form as flows slow during falling river flood stages (Best et al. 2003). Herringbone cross-beds can develop locally in fluvial settings where flow reversals occur at channel confluences or in flow separation zones in the lee of bars (Long 2006). Reactivation surfaces without any evidence of subordinate currents can be produced by unidirectional flow systems, such as fluvial channels (Nio and Yang 1991), and sigmoidal cross-stratification can be the result of a progressive increment of flow velocity within fluvial channels (Roe 1987). Preservation of mud drapes within cross-sets of Facies 1 and small-scale cross-stratification observed on top of the bar deposits could form following channel avulsion and/or migration (Bristow and Best 1993). The abundance of these features, however, strongly suggests the influence of tidal processes on deposition.

Facies variations within bedsets, and the lateral stacking of different bedsets, suggest that these are deposits of migrating dunes and shallow-water bars. The distinction between fluvial channel and less laterally confined shallow marine bars can be difficult in deposits of this age strata, where ichnological evidence is sparse. The dominate grain size of medium to coarse sand suggests rapid flows. Bedsets that terminate into channel fills with steeper "cutbank" margins suggest channelized flows, whereas those that grade laterally from sandier erosionally-based to muddier Facies without clear evidence of basal erosion probably record less confined flows. Dominant evidence for unidirectional flow directions within individual bedsets favors deposition within fluvial channels. Conversely, in Cambrian-aged deposits the presence of bioturbation is an unambiguous indication of deposition in marine waters. Taken together the evidence suggests a mix of coastal river deposits and shallow marine deposits.

Evidence for rapid currents and dominantly unidirectional flows are interpreted to reflect a dominance of outflow processes characteristic of river-influenced delta. Channel deposits that have a basal erosion surface and terminate laterally at cutbank margins, display high width to thickness ratios characteristic of relatively straight channels. The relative length of bar accretion deposits (Facies 1 and 2) to muddier channel fill deposits (Facies 3) within individual bedsets also indicates relatively straight channels. Convex-upward beds in the center of some bedsets provide strong evidence of braided channel patterns. The high proportion of channel-fill deposits relative to lateral accretion deposits and the occurrence of many sandy channel fills (versus mudstone-dominated plugs) also supports braided channel interpretations (Bridge 1985). Although the complex stacking of low sinuosity channel deposits is a common product of rivers with high avulsion frequency, in this case this depositional pattern can also be inferred to reflect flashy discharge.

Braided, highly-mobile, bedload-dominated distributary channels closely spaced along the shoreline would feed the delta front essentially as a line source (Postma 1990). In contrast to many modern highstand river-dominated delta mouth bars, those in the Hickory Sandstone do not appear to rapidly thicken away from terminating distributary channels. In the shallow waters along the edge of an epicontinental sea turbulent diffusion would have been dominately horizontal and bottom friction would thus have played a major role in effluent deceleration and expansion (Coleman 1980; Postma 1990; Boggs 2001). Rapid effluent expansion would result in depositional broad radial bars (Coleman 1980), where coarser-sands were deposited at the channel mouth and finer-grained sediments in areas farther seaward. Preferential occur of bioturbation within finer grained deposits may in part reflect this more marine depositional position. An initial mouth bar deposited close to the channel axis could deflect and split the flow, causing the channel to bifurcate (Axelsson 1967; Coleman 1980; Postma 1990; Olariu and Bhattacharya 2006). The development of these two new channels defines the initial formation of a "terminal" distributary channel (sensu Olariu and Bhattacharya 2006). This channel bifurcation is followed by the growth and migration of new mouth bars. Progressive mouth-bar accretion can evidentially block new distributary channel bifurcation, resulting in a larger-scale distributary channel abandonment (Olariu and

Bhattacharya 2006). After abandonment, areas with mouth bars may continue to subside and become covered with more quiescent marine Facies.

Deposition of the lower Hickory Sandstone was controlled by two paleographic features: 1) the existence of a shallow and wide epicontinental sea, and 2) the ridge-and-swale topography formed by differential erosion of the folded, less resistant Precambrian schists and more resistant Precambrian gneisses prior to Hickory Sandstone deposition. Both these features are expected to enhance tidal currents. As tidal waves move from the open ocean onto a wide, shallow water platform, their cross-sectional area is reduced, increasing tidal range (Dalrymple 1992; Eriksson and Reckzo 1998). As the seas transgressed, the ridge-and-swale topography would have defined shoreline embayments in which the tidal range was further increased. Uplands within this landscape would have supplied the relativly coarse sediments observed in the lower Hickory. These coarse-grained sediments were probably too coarse to be completely reworked by tidal currents, hindering full development of distinctive tidal-influenced depositional features. It may also be that most mud deposits in this succession formed after an area on the delta was abandoned, in contrast to modern tidal systems where clouds of flocculated muds commonly travel with sands under tidal currents.

Assuming the very gentle slope of an epicontinental sea floor predicted by Irwin (1965), dissipation or damping of open ocean waves (greater than a few meters in height) would have occurred within a 100 km of the continental shelf edge (Eriksson and Reckzo 1998). The lack of hummocky cross-stratification or frequent symmetrical ripples suggests that Hickory deposition was inboard of areas strongly influenced by the oscillatory currents produced by open ocean waves. Paleotopographic bays or inlands could have also caused refraction, further defusing wave energy.

The depositional environment of the lower Hickory is interpreted to be a braid-delta system fed by low-sinuosity bedload-dominated rivers (Fig. 22). Low offshore gradients along the edge of an epicontinental sea resulted in very gradual transitions from channelised fluvial flows to less confined decelerating flows around marine mouth bars. Mudstones containing the bioturbation indicate deposition in marine waters, and unlike modern environments it is unclear that there was life in marginal marine areas where a salt wedge extend into distributary channels (MacEachern et al. 2005). Regressions and transgressions are difficult to recognize because low suspended sediment loads resulted in slow accumulation of marine muds as flows moved offshore. Flashy river discharge and frequent channel avulsion resulted in similar accumulations of muds as areas were abandoned along depositional strike. The lack of land vegetation probably resulted in high rates of sediment supply and thus coarse-grained sediments, which dampened the influence of basin currents along the coast. Low suspended sediment load also suppressed preservation of classic tidal features during pauses in tidal currents. This low gradient setting also dampened waves along the shoreline.

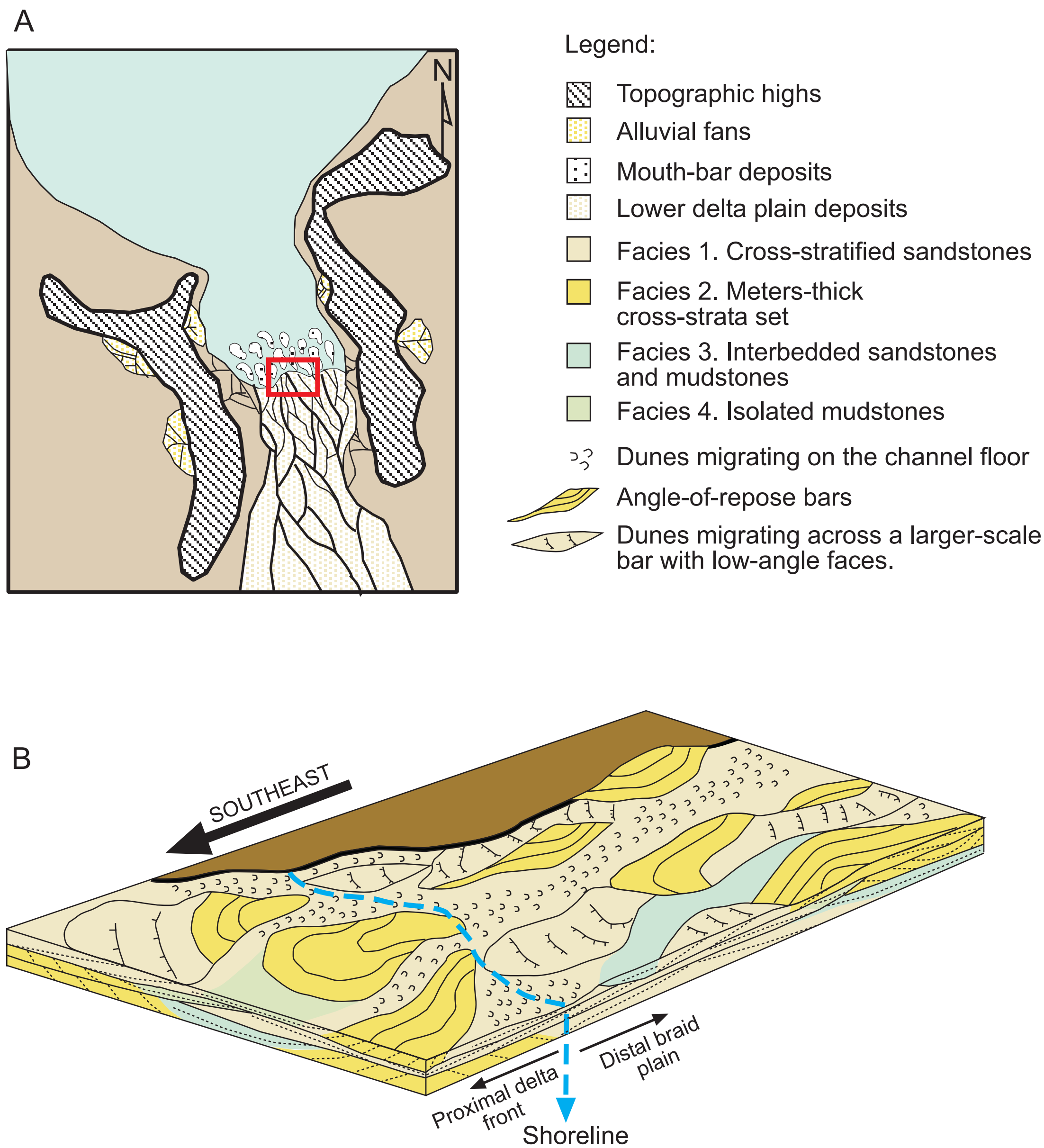

Fig. 22. Conceptual sedimentological model proposed for this study. A) Plan view showing the braid-delta system fed by low-sinuosity rivers. Area of deposition is indicated by the red box. B) Diagram showing idealized distribution of facies within the depositional environment.

CONCLUSION

Hickory Sandstone deposits exposed in the study area are dominated by sheet-like bodies composed internally of four main Facies: 1) cross-stratified sandstones; 2) meters-thick cross-strata sets; 3) interbedded sandstones and mudstones; and 4) isolated mudstones. Lateral Facies assemblages were used to define four bedsets types, which are superposed laterally creating a complex alternation of sandstone- and mudstone-dominated deposits. The architecture of these deposits, internal distribution of Facies, and patterns bioturbation reflect deposition in the transition from the lower delta plain to the proximal delta front of a river-influenced delta. The absence of vegetation resulted in highly variable discharge, high rates of sediment supply and low bank stability normally associated with braided channel patterns. These low-sinuosity braided distributary channels, hundreds of meters wide and few meters deep, debouched into a very shallow epicontinental sea. Depositional conditions within this shallow sea, together with the ridge-and-swale paleotopography, dissipated wave influence at the shoreline and enhanced tidal currents, as indicated by the local occurrence of mud drapes, concave-upward cross-strata and sparse reactivation surfaces and herringbone cross-stratification. This succession records the transition from the fluvial-dominated deposits of the lower Hickory to marine-influenced deposits of the middle Hickory, within an overall transgressive sequence.

REFERENCES

Allen, J.R.L., 1983, Studies in fluviatile, sedimentation: bars, bar-complexes and sandstone sheets (low sinuosity braided-streams) in the Brownstone (L. Devonian), Welsh Borders: Sedimentary Geology, v. 33, p. 237-293.

Amireh, B.S., Schneider, W., and Abed, A.M., 1994, Evolving fluvial-transitional-marine deposition through the Cambrian sequence of Jordan: Sedimentary Geology, v. 89, p. 65-90.

Axelsson, V., 1967, The Laitaure Delta, a study of deltaic morphology and processes: Geogr. Ann., v. 49A, p. 1-127.

Barnes, V.E. and Bell W.C., 1977, The Moore Hollow Group of Central Texas: The University of Texas at Austin, Bureau of Economic Geology, Report of Investigations no. 88, 169 p.

Barnes, V.E. and Schofield D.A., 1964, Potential low-grade iron ore and hydraulic fracturing sand in Cambrian sandstones, northwestern Llano region, Texas: The University of Texas at Austin, Bureau of Economic Geology, Report of Investigations no. 53, 58 p.

Barnes, V.E., Cloud, P.E., Jr., Dixon, L.P., Folk, R.L., Jonas, E.C., Palmer, A.R., and Tynan, E.J., 1959, Stratigraphy of the pre-Simpson Paleozoic subsurface of Texas and southeast Nex Mexico: The University of Texas, Austin, Bureau of Economic Geology, Publication No. 5924, 2 vols., 836 p. + 65 pls.

Berner, R.A., 1993, Paleozoic atmospheric CO2: importance of solar radiation and plant evolution: Science, v.261, p. 68-70.

Best, J.L., Ashworth, P.J., Bristow, C., and Roden, J., 2003, Three-dimensional sedimentary architecture of a large, mid-channel sand braid bar, Jamuna River, Bangladesh: Journal of Sedimentary Research, v. 73, p. 516-530.

Bhattacharyya, A., and Chakraborty C., 2000, Analysis of Sedimentary Successions: a Field Manual: Rotterdam, The Netherlands, Balkema Publishers, 408 p.

Blakey, R., Paleogeography and geologic evolution of North America, Information consulted in March 2006, (http://jan.ucc.nau.edu/~rcb7/nam.html).

Boggs, S., 2001, Principles of Sedimentology and Stratigraphy: Upper Saddle River, NJ, Prentice Hall, 726 p.

Bouma, A.H., Brenner, R.L., and Knebel, H J., 1982, Continental shelf and epicontinental seaway, in Scholle, P. A. and Spearing, D., eds., Sandstone Depositional Environments: American Association of Petroleum Geologist, Tulsa, p. 281-327.

Brenner, R.L., 1980, Construction of process-response models for ancient epicontinental seaway depositional systems using partial analogs: Bull. Am. Ass. Petrol. Geol., v. 64, p. 1223-1244.

Bridge, J., Barnes V.E. and Cloud Jr. P.E., 1947, Stratigraphy of the Upper Cambrian, Llano Uplift, Texas: GSA Bulletin, v. 58, no. 1, p. 109-123.

Bridge, J.S., 1985, Paleochannel patterns inferred from alluvial deposits: a critical evaluation: Journal of Sedimentary Petrology, v. 55, p. 579-589.

Bridge, J.S., 1993a, The interaction between channel geometry, water flow, sediment transport and deposition in braided rivers, in Best, J.L., Bristow, C.S., eds., Braided Rivers: Geol. Soc. London, Special Publication 75, p. 13-71.

Bridge, J.S., 1993b, Description and interpretation of fluvial deposits: a critical perspective: Sedimentology, v. 40, p. 801-810.

Bristow, C.S., and Best, J.L., 1993, Braided Rivers, perspective and problems, in Best, J.L. and Bristow, C.S., eds., Braided Rivers: Geol. Soc. London, Spec. Publ. 75, p. 1-11.

Chakraborty, C., and Bose, P.K., 1992, Ripple/dune to upper stage plane-bed transition: some observations from the ancient record. Geol. J., v. 27, p. 349–359.

Cloud, P.E. Jr., Barnes V.E., and Bridge J., 1945, Stratigraphy of the Ellenburger group in central Texas: a progress report: The University of Texas Pub. 4301, The University of Texas at Austin, Bureau of Economic Geology, p. 133-161.

Coleman, J.M., 1980, Deltas: Processes of Deposition and Models for Exploration: second edition, Minneapolis, MN, Burgess, 124 p.

Cornish, F.G., 1975, Tidally-influenced deposits of the Hickory Sandstone, Cambrian, central Texas: M.S. thesis, The University of Texas, Austin, TX, 186 p.

Cotter, E., 1978, The evolution of fluvial style, with special reference to the central Appalachian Paleozoic., in Miall, A.D., eds., Fluvial Sedimentology: Can. Soc. Pet. Geol. Mem. 5, p. 361–383.

Dalrymple, R. W., 1992, Tidal depositional systems, in Walker R.G., and James, N.P., eds., Facies Models: Response to Sea Level Change: St. John’s, Nfld., Geologic Association of Canada, p. 195-218.

Dalrymple, R.W., Narbonne, G.M., and Smith L., 1985, Eolian action and the distribution of Cambrian shales in North America. Geology, 13, p. 607-610.

Dalziel, I.W., and Gahagan, L.M., 2006, The making of Texas, Information consulted in March 2006. (http://www.ig.utexas.edu/research/projects/plates/posters/Making_of_Texas_08aug2006.pdf)

Eriksson, P.G., and Reczko, B.F.F., 1998, Contourites associated with pelagic mudrocks and distal delta-fed turbidites in the Lower Proterozoic Timeball Hill Formation epeiric basin (Transvaal Supergroup), South Africa: Sedimentary Geology, v. 120, p. 319–335.

Eriksson, P.G., Altermann, W., Eberhardt, L., Arend-Heidbrinck, S., and Bumby, A.J., 2002, Paleoproterozoic epeiric sea palaeoenvironments: The Silverton Formation (Pretoria Group, Transvaal Supergroup), South Africa, in Altermann, W., and Corcoran, P., eds., Precambrian Sedimentary Environments: A Modern Approach to Ancient Depositional Systems: Special Publication International Association of Sedimentologists 33, p. 351-367.

Eriksson, P.G., Condie, K.C., Tirsgaard, H., Mueller, W.U., Altermann, W., Miall, A.D., Aspler, L.B., Catuneanu O., and Chiarenzelli, J.R., 1998, Precambrian clastic sedimentation systems: Sedimentary Geology, v. 120, p. 5-53.

Eriksson, P.G., Reczko, B.F.F., Boshoff, A.J., Schreiber, U.M., Van der Neut, M., and Snyman, C.P., 1995, Architectural elements from Lower Proterozoic braid-delta and high-energy tidal flat deposits in the Magaliesberg Formation, Transvaal Supergroup, South Africa: Sediment. Geol., v. 97, p. 99–117.

Goolsby, J.L., 1957, A study of the Hickory Sandstone: M.S. Thesis, Texas A&M University, College Station, TX, 92 p.

Haddox, C.A., and Dott, R.H., 1990, Cambrian shoreline deposits in northern Michigan: Jour. Sed. Petrology, v. 60, p. 697-716.

Hiscott, R.N., Noel, J.P., and Pemberton, S.G., 1984, Sedimentology and ichnology of the Lower Cambrian Bradore Formation, coastal Labrador; fluvial to shallow-marine transgressive sequence: Bulletin of Canadian Petroleum Geology, v. 32, p. 11-26.

Irwin, M.L., 1965, General theory of epeiric clear water sedimentation: Bull. Am. Ass. Petrol. Geol., v. 49, p. 445-459.

Jensen, S. 2003. The Proterozoic and earliest Cambrian trace fossil record; patterns, problems and perspectives: Integr. Comp. Biol., v. 43, p. 219-228.

Johnson, B., 1997, Fluid-flow properties of faults and field-scale studies of faulted reservoirs: in Industrial Associates Program: Center for Tectonophysics, Texas A&M University, p. 3-13.

Keulegan, G.H. and Krumbein, W.C. 1949. Stable configuration of bottom slope in a shallow sea and its bearing on geological processes. Transactions, American Geophysical Union, 30, 855–861.

Kim, Y., 1995, Aquifer mineralogy and natural radionuclides in groundwater: the lower Paleozoic of central Texas: M. S. thesis, Texas A&M University, College Station, TX. 126 p.

Knighton, D., 1984, Fluvial Forms and Processes. Edward Arnold: London.

Krause, S.J., 1996, Stratigraphic framework, Facies analysis, and depositional history of the Middle to Late Cambrian Riley Formation, central Texas: M.S. thesis, The University of Texas, Austin, TX, 172 p.

Long, D.G.F., 2006, Architecture of pre-vegetation sandy-braided perennial and ephemeral river deposits in the Paleoproterozoic Athabasca Group, northern Saskatchewan, Canada as indicators of Precambrian fluvial style: Sedimentary Geology, v. 190, p. 71-95.

MacEachern, J.A., Bann, K.L., Bhattacharya, J.P., and Howell, C.D., 2005, Icnology of deltas: Organism responses to the dynamic interplay of rivers, waves, storms and tides, in Giosan, L., and Bhattacharya, J.P., eds., River Deltas: Concepts, Models, and Examples: SEPM, Special Publication 83, p. 49-85.

Macnaughton, R., Dalrymple, R., and Narbonne, G., 1997, Early Cambrian braid delta deposits, MacKenzie Mountains, north western Canada: Sedimentology, v. 44, p. 587-609.

Mazumber, R., 2003, Sediment transport, aqueous bedform stability and morphodynamics under unidirectional current: a brief overview: J. African Earth Sci., v. 36, p. 1-14

McBride, E.F., Abdel-Wahab, A.A. and Milliken, K.L., 2002, Petrography and diagenesis of a half-billion-year-old cratonic sandstone (Hickory), Llano region, Texas: The University of Texas, Austin, Bureau of Economic Geology, Report of Investigation No. 264, 77 p.

McCormick, D.S. and Grotzinger, J.P., 1993, Distinction of marine from alluvial Facies in the Paleoproterozoic (1.9 Ga) Burnside Formation, Kilohigok Basin, N.W.T., Canada: J. Sediment. Petrol., v. 63, p. 398–419.

Miall, A.D., 1985, Architectural-element analysis: a new method of Facies analysis applied to fluvial deposits: Earth Sci. Rev., v. 22, p. 261-308.

Miller, M.F., 1984, Distribution of biogenic structures in Paleozoic nonmarine and marine-marginal sequences: an actualistic model, J. Paleontology, v. 58, p. 550-570.

Nio, S.D., and Yang, C.S., 1991, Diagnostic attributes of clastic tidal deposits: a review, in Smith, D.G., Reinson, G.E., Zaitlin, B.A, and Rahmani, R.A., eds., Clastic Tidal Sedimentology: Canadian Society of Petroleum Geologists, Memoir 16, p. 3–28.

Olariu, C., and Bhattacharya, J.P., 2006, Terminal distributary channels and delta front architecture of river-dominated delta systems: Journal of Sedimentary Research, v. 76, p. 212-233.

Postma, G., 1990, Depositional architecture and Facies of rivers and fan deltas: a synthesis, in Colella, A., and Prior D.B., eds., Coarse Grained Deltas: Spec. Publs. Int. Ass. Sediment. 10, p. 13-27.

Randolph, L.C., 1991, The effects of faults on the groundwater system in the Hickory Sandstone aquifer in central Texas: M.S. thesis, Texas A&M University, College Station, TX, 102 p.

Roe, S., 1987. Cross-strata and bedforms of probable transitional dune to upper stage plane bed origin from a Late Precambrian fluvial sandstone, northern Norway. Sedimentology, 34, p. 89–101.

Røe, S.-L. and Hermansen, M., 1993, Processes and products of large, late Precambrian sandy rivers in northern Norway., in Marzo, M., Puigdefábregas, C., eds., Alluvial Sedimentation: Spec. Publ. Int. Assoc. Sedimentol., 17, p. 151–166

Schumm. S.A., 1985, Patterns of alluvial rivers. Annu. Rev. Earth Planet. Sci. v. 13. p. 5-27.

Smith, D.G., 1976, Effect of vegetation on lateral migration of anastomosed channels of a glacial meltwater river. Geol. Soc. Am. Bull. 87, p. 209–230

Soegaard, K., and Eriksson, K.A., 1989, Origin of thick, first-cycle quartz arenite successions: evidence from the 1.7 Ga Ortega Group, Northern New Mexico. Precambrian Res., v. 43, 129–141.

Sønderholm, M., and Tirsgaard, H., 1998, Proterozoic fluvial styles: response to changes in accommodation space (Rivieradal sandstones, eastern North Greenland), Sedimentary Geology, v. 120, p. 257-274.

Stenzel, H.B., 1935, Precambrian structural conditions in the Llano region: in v.2 of the geology of Texas: The University of Texas at Austin Bulletin 3401, p. 74-79.

Tape, C., Clinton, H., Cowan, A. and Runkel, A.C., 2003, Tidal-bundle sequences in the Jordan Sandstone (Upper Cambrian), southeastern Minnesota, U.S.A.: evidence for tides along inboard shorelines of the Sauk epicontinental sea, Journal of Sedimentary Research, v. 73, p. 354-366.

Tirsgaard, H., 1993, The architecture of Precambrian high energy tidal channel deposits: an example from the Lyell Land Group (Eleonore Bay Supergroup), northeast Greenland. Sediment. Geol., v. 88, p. 137–152.

Willis B.J., 1997, Architecture of a fluvial-dominated valley-fill deposits in the Cretaceous Fall River: Sedimentology, v. 44, p. 735-757.

Willis B.J., J.P. Bhattacharya, S.L. Gabel, and C.D. White, 1999, Architecture of a tide-influenced delta in the Frontier Formation of central Wyoming: Sedimentology, v. 46, p. 667-688.

Wilson, J.S., 2001, High-resolution stratigraphic and structural characterization of the fault-partitioned hickory sandstone aquifer system, Mason County, central Texas: M.S. thesis, Texas A&M University, College Station, TX. 151 p.

Wilson, W.F., 1962, Sedimentary petrology and sedimentary structures of the Cambrian Hickory Sandstone Member, Central Texas: M.S. thesis, The University of Texas at Austin, 229 p.

VITA

Isaac Antonio Perez Teran received his Bachelor of Science degree in geological engineering from Universidad de los Andes, Merida, Venezuela , in July of 2003. He began his graduate studies in geology at Texas A&M University in August of 2004, and received his Master of Science degree in August of 2007. His research interests include analysis of sedimentary sequences in order to define different sedimentary processes and depositional environments.

Mr. Perez may be reached at the Department of Geology and Geophysics at Texas A&M University, College Station, TX 77843. His email address is isaacperezteran@yahoo.com.